JGR Biogeosciences

RESEARCH ARTICLE
10.1029/2023JG007401

Particulate Organic Matter in the Atacama Trench: Tracing Sources and Possible Transport Mechanisms to the Hadal Seafloor

Edgart Flores[1,2,3], Igor Fernández-Urruzola[2], Sebastian I. Cantarero[4], Matías Pizarro-Koch[5,6], Matthias Zabel[7], Julio Sepúlveda[2,4], and Osvaldo Ulloa[1,2]

[1]Departamento de Oceanografía, Facultad de Ciencias Naturales y Oceanográficas, Universidad de Concepción, Concepción, Chile, [2]Millennium Institute of Oceanography, Universidad de Concepción, Concepción, Chile, [3]Now at Department of Geological Sciences, Institute of Arctic and Alpine Research, University of Colorado Boulder, Boulder, CO, USA, [4]Department of Geological Sciences, Institute of Arctic and Alpine Research, University of Colorado Boulder, Boulder, CO, USA, [5]Millennium Nucleus Understanding Past Coastal Upwelling Systems and Environmental Local and Lasting Impacts, Coquimbo, Chile, [6]Escuela de Ingeniería Civil Oceánica, Facultad de Ingeniería, Universidad de Valparaíso, Valparaíso, Chile, [7]MARUM—Center for Marine Environmental Sciences and Department of Geosciences, University of Bremen, Bremen, Germany

Abstract Oceanic trenches are an important sink for organic matter (OM). However, little is known about how much of the OM reaching the hadal region derives from the sunlit surface ocean and other sources. We provide new insight into the OM sources in the Atacama Trench by examining the elemental and stable isotope composition of carbon and nitrogen in bulk OM throughout the entire water column and down to bathyal and hadal sediments. Moreover, we estimated the particulate organic carbon (POC) concentration and downward carbon flux. Our results, based on two-way variance analysis, showed statistical differences in $\delta^{15}N_{PON}$ between the epipelagic zone and the deep zones. However, no statistical differences in $\delta^{13}C_{POC}$ and C:N ratio between hadalpelagic and shallower pelagic zones were found, except for $\delta^{13}C_{POC}$ in the oxygen-deficient zone. On the contrary, whereas the isotopic signatures of hadal sediments were distinct from those over the entire water column, they were similar to the values in bathyal sediments. Thus, our results suggest that bathyal sediments could contribute more OM to hadal sediments than the different zones of the water column. Indeed, whereas POC flux estimates derived from remote sensing data indicate that ~16%–27% of POC could evade surface remineralization within the top 200 m and potentially be exported to depths beyond the mesopelagic region, model estimates suggest that ~3.3% of it could reach hadal depths. Our results provide a quantitative baseline of pelagic-benthic coupling which can aid in assessment of carbon cycling changes in future climate scenarios.

Plain Language Summary Hadal trenches (>6,000 m) represent the deepest part of the ocean and are an important sink for organic matter (OM). This OM is an important energy source for heterotrophic microbes living in hadal sediments and consequently for the recycling of nutrients. However, the mechanisms of how this material reaches the hadopelagic zone as well as the relative contributions from diverse sources remain poorly understood. The carbon and nitrogen stable isotope compositions of bulk OM have been widely used to elucidate the relative contribution of OM sources in the ocean. However, few studies have evaluated the isotopic composition of particulate organic matter from surface waters all the way to the hadopelagic region and surface hadal sediments. We conclude that whereas the hadopelagic water column receives <12% of OM from the sunlit shallow ocean, only ~3% reaches the hadal benthic zone, which receives a larger contribution from downslope sediment transport. Our results provide new insights in the cycling of carbon between the upper and deep ocean, which can assist with the forecasting of potential changes under progressive climate forcing.

Key Points:

- The deep-sea waters of the Atacama Trench display bulk isotopic signatures in the particulate organic matter (POM) similar to those in the epipelagic zone
- The bulk and stable isotope composition of POM in surface bathyal and hadal sediments is distinguishable from the one in the water column
- A stable isotope model suggests that hadal sediments may receive more organic matter from shallower-water sediments than from the water column

Supporting Information:

Supporting Information may be found in the online version of this article.

Correspondence to:

E. Flores and O. Ulloa,
edgart.flores@imo-chile.cl;
oulloa@udec.cl

Citation:

Flores, E., Fernández-Urruzola, I., Cantarero, S. I., Pizarro-Koch, M., Zabel, M., Sepúlveda, J., & Ulloa, O. (2023). Particulate organic matter in the Atacama Trench: Tracing sources and possible transport mechanisms to the hadal seafloor. *Journal of Geophysical Research: Biogeosciences*, *128*, e2023JG007401. https://doi.org/10.1029/2023JG007401

Received 20 JAN 2023
Accepted 29 JUL 2023
Corrected 28 AUG 2023

This article was corrected on 28 AUG 2023. See the end of the full text for details.

Author Contributions:

Conceptualization: Igor Fernández-Urruzola, Sebastian I. Cantarero, Julio Sepúlveda, Osvaldo Ulloa

1. Introduction

Most marine particulate organic matter (POM) produced at the ocean's surface is remineralized in its descent through the water column to the seafloor, resulting in a particle flux attenuation with increasing water depth (Hedges et al., 2001; Rex et al., 2006; Wakeham et al., 1984) that generally follows a simple power-law function (Martin et al., 1987). Both the magnitude of the export production and the remineralization depth of the sinking material determine the shape of the attenuation curve and, ultimately, the amount of POM that reaches the sediment surface and supplies energy to deep-sea communities. POM varies in size and composition, ranging

Funding acquisition: Igor Fernández-Urruzola, Julio Sepúlveda, Osvaldo Ulloa
Investigation: Julio Sepúlveda, Osvaldo Ulloa
Methodology: Igor Fernández-Urruzola, Sebastian I. Cantarero, Julio Sepúlveda, Osvaldo Ulloa
Project Administration: Osvaldo Ulloa
Supervision: Julio Sepúlveda, Osvaldo Ulloa
Writing – original draft: Igor Fernández-Urruzola, Sebastian I. Cantarero, Julio Sepúlveda
Writing – review & editing: Igor Fernández-Urruzola, Sebastian I. Cantarero, Matías Pizarro-Koch, Matthias Zabel, Julio Sepúlveda, Osvaldo Ulloa

from phytodetritus (Rice et al., 1986), larvacean houses (Robison et al., 2005) and faecal pellets (Turner, 2002) to mucilaginous aggregates (Martín & Miquel, 2010). The downward flux of organic material is further affected by the regional and seasonal variability in export flux (de Melo Viríssimo et al., 2022; Lutz et al., 2007; Poff et al., 2021), the size, shape, and composition of the POM (De La Rocha et al., 2008; Kriest, 2002; Omand et al., 2020), the interaction with microbes and/or zooplankton (Cavan et al., 2021; Neubauer et al., 2021), physical processes of aggregation/disaggregation of particles (Burd & Jackson, 2009; Iversen & Ploug, 2010), and ventilation/advection through deep-ocean circulation (Chunhui et al., 2020). According to biogeochemical models (e.g., Ichino et al., 2015), the export of sinking OM of photosynthetic origin to hadal depths (>6,000 m below sea level) is expected to be low. However, oceanic trenches have been described as depocenters of OM (Danovaro et al., 2003) and hotspots for heterotrophic microbial activity (Glud et al., 2013; Liu et al., 2019; Luo et al., 2018; Wenzhöfer et al., 2016). The coupling between microbial activity and OM availability is important for nutrient remineralization, which can in turn influence the rates and directions of biogeochemical fluxes (Azam et al., 1994). Thus, elevated concentrations of OM in trench sediments could be explained by more diverse sources of energy feeding the hadal environment. Besides the downward flux of particulate organic carbon (POC) from surface waters, processes such as the carrion falls of dead bodies, terrestrial inputs from the adjacent continental margin, in situ chemosynthetic production, and the lateral transport of sediment along the continental slope may potentially provide OM to these remote ecosystems (Flores et al., 2022; Xu et al., 2018). However, their relative contribution to the total carbon supply to the hadal region remains poorly constrained. Whereas recent research has linked hadal benthic microbial activity to regional productivity of the overlying surface waters (Glud et al., 2021; Luo et al., 2018), differences in calculated POM export from the productive sunlit surface ocean do not explain, by themselves, why hadal sediments consistently indicate greater biological activity than their shallower adjacent abyssal sites. Moreover, whether this biogeochemical activity pattern in the trench sediments can also be extrapolated to the pelagic environment is unknown.

The Atacama Trench in the eastern tropical South Pacific (ETSP) is overlaid by a eutrophic water column compared to other trench ecosystems in the Pacific Ocean underling mesotrophic (e.g., Japan and Izu-Bonin Trenches) and oligotrophic waters (e.g., Mariana and Tonga Trenches) (Wenzhöfer et al., 2016). This trench underlies the Humboldt Current System, one of the world's most productive coastal upwelling ecosystems characterized by a large, permanent and intense oxygen minimum zone (OMZ; Daneri et al., 2000; Fuenzalida et al., 2009; Selden et al., 2021). Empirical estimates of export fraction and flux attenuation in the water column overlaying the Atacama Trench have demonstrated that the export production may sustain most of the respiratory carbon demand of the plankton community across the hadalpelagic zone (Fernández-Urruzola et al., 2021). These authors hypothesized that fast-sinking particles represent an important mechanism for the injection of fresh POM into hadal depths, since large particles such as diatom aggregates and fecal pellets may more easily escape from remineralization in the upper ocean (González et al., 2000; Grabowski et al., 2019). Other physical and chemical processes likely play an additional role in the downward flux of POM to hadal depths in the region; for instance, eddy-driven subduction events can rapidly transfer carbon in pulses below the mixed layer (Omand et al., 2015; Resplandy et al., 2019). Moreover, the presence of an OMZ can also impact carbon cycling and fluxes to the ocean's interior acting as a secondary biological pump, and providing an additional source of freshly produced OM to the ocean's interior (Pantoja et al., 2004; Devol & Hartnett, 2001; Van Mooy et al., 2002; Weber & Bianchi et al., 2020). A study of the distribution and abundance of intact polar lipids (IPLs) in POM of the OMZ system over the Atacama Trench suggested that chemosynthetic processes associated with dark carbon fixation provide additional sources of organic carbon to the mesopelagic region (Cantarero et al., 2020). These results were later confirmed by quantitative estimates using a stable isotope mass-balance (Vargas et al., 2021), which indicated that dark carbon fixation in OMZ waters contributes ~7%–35% of the total POC exported to mesopelagic waters. While little is known about how much of this OM reaches the hadalpelagic realm, the distribution and abundance of IPLs in hadal surface sediments of the Atacama Trench points to the importance of in situ microbial biomass production as a key source of labile OM in this hadal environment (Flores et al., 2022). These authors demonstrated that IPLs in hadal and bathyal sediments show close resemblance, and that they are distinguishable from the IPLs previously reported in the overlying water column (Cantarero et al., 2020). Thus, discrepancies remain among measurements of carbon accumulation in sediments, the vertical POC flux, and in situ production of hadal OM (Flores et al., 2022; Oguri et al., 2022; Turnewitsch et al., 2014), as well as between the dominant terrigenous versus marine carbon sources even within the same trench (e.g., Atacama Trench; Xu et al., 2021; Oguri et al., 2022).

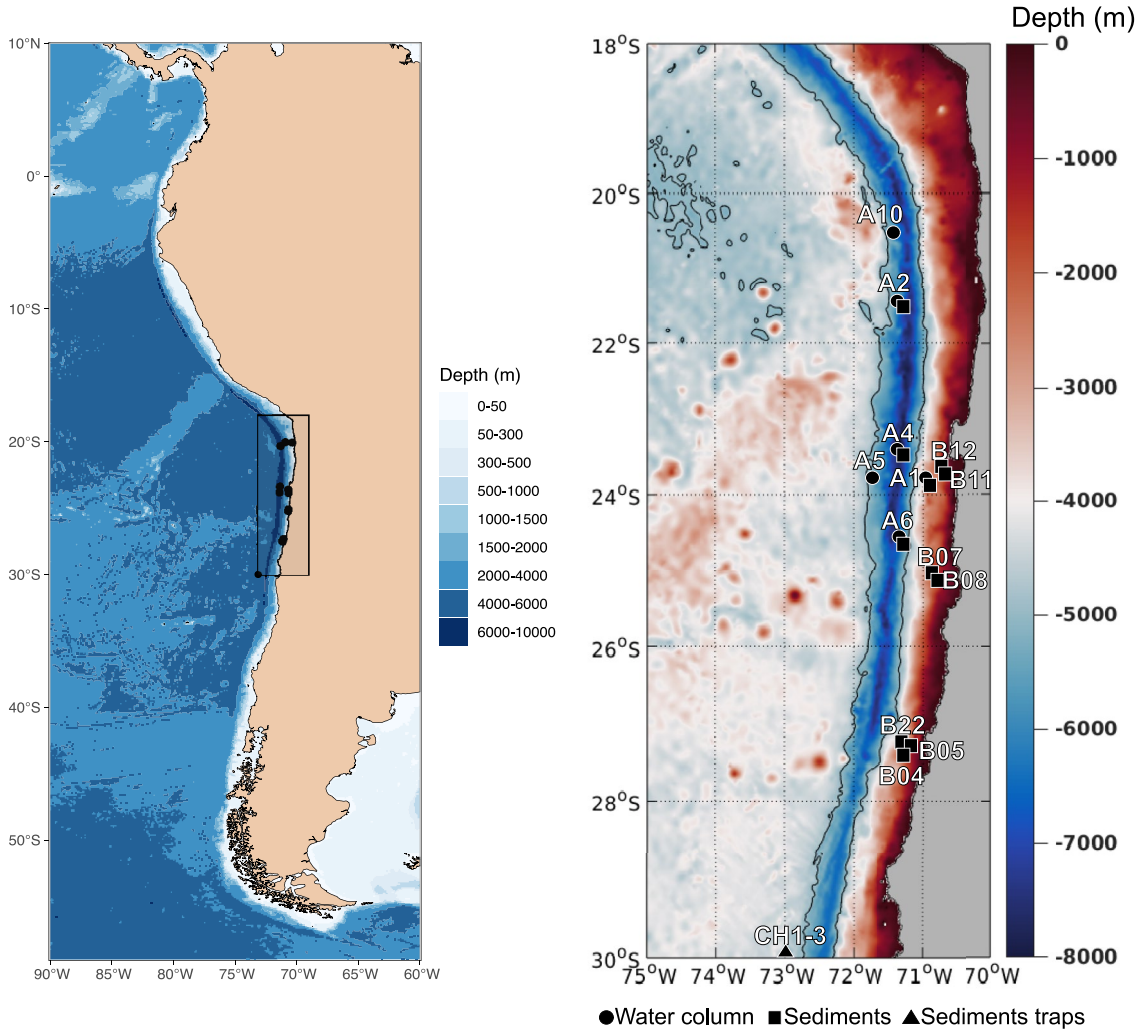

Figure 1. Study area. (a) Bathymetric map of the eastern south Pacific Ocean showing the study area in the Atacama Trench region off northern Chile (black rectangle). (b) Bathymetric map of the study area showing the sampling stations.

The carbon and nitrogen stable isotope compositions of bulk OM have been widely used to elucidate the relative contribution of OM sources (Gao et al., 2012; Meyers & Eadie, 1993; Middelburg & Nieuwenhuize, 1998), including hadal sediments from the Mariana Trench (Luo et al., 2019), the New Britain Trench (Xiao et al., 2020), and the Atacama and Kermadec Trenches (Xu. et al., 2021). However, few studies have evaluated the isotopic composition of POM from surface waters to the trench interior, including the hadalpelagic region and the surface sediments. Here, we investigate the provenance and fate of sinking particles across the epipelagic (<200 m), mesopelagic (200–1,000 m), oxygen-deficient (60–500 m), bathypelagic (1,000–3,500 m), abyssopelagic (3,500–6,000 m), and hadalpelagic (>6,000 m) zones, following the depth zonation of Jamieson (2015, and references therein), as well as the sedimentary material at the deepest points of the Atacama Trench (7,734–8,063 m).

2. Materials and Methods

2.1. Study Area and Sample Collection

Water column samples were collected at four sites between 21° and 24°S over the Atacama Trench during the SO261 cruise (HADES, 2 March to 2 April 2018, Wenzhöfer, 2019) on board the German RV *Sonne* (Figure 1; Table 1). We obtained seawater from eight discrete depths down to 6,000 m using a rosette sampler with 24 12L-Niskin bottles. Additionally, we collected samples from 1.5 m above the seafloor using an autonomous

Journal of Geophysical Research: Biogeosciences

10.1029/2023JG007401

Table 1
Sampling Stations From the HADES and ChiMeBo Cruises, and From Published Sediment-Trap Data

Environment	Cruise-RV	Station	Samples type	Depth (m)	Latitude (°S)	Longitude (°W)	Date (dd/mm/yyyy)	Reference
Water column	HADES Sonne SO261	A1	Epipelagic (5, 20, 60, 200 m) Mesopelagic (500, 1,000 m)	2,560	23.81	70.84	05/03/2018	This study
		A2	Epipelagic (5, 20, 60, 200 m) Mesopelagic (500, 1,000 m), Bathypelagic (2,000, 3,000, 4,000 m) Abysopelagic(5,000, 6,000 m), hadalpelagic (>6,000 m)	7,994	21.78	71.21	25/03/2018	
		A4		8,086	23.36	71.34	14/03/2018	
		A6		7,720	24.27	71.42	09/03/2018	
	Vidal Gormaz	CH1-3	Bathypelagic depth sediment trap	2300, 3,700	30	73.18	21/07/1993	Hebbeln et al. (2000)
	Abate Molina	–		2300	30	73.18	07/1993–05/1995	Gonzalez et al., (2004)
Sediments	HADES Sonne SO261	A10	Hadal sediments (0–1, 1–2 and 2–3 cm)	7,734	20.32	71.29	26/03/2018	This study
		A5	Hadal sediments (0–1, 1–2 and 2–3 cm)	7,890	23.81	71.37	11/03/2018	
		A4	Hadal sediments (0–1, 1–2 and 2–3 cm)	8,063	23.36	71.34	14/03/2018	
	ChiMeBo Sonne SO211	B12	Upper bathyal sediment (0–1 cm)	529	23.59	70.67	02–29/11/2010	This study
		B08	Upper bathyal sediment (0–1 cm)	539	25.2	70.68	02–29/11/2010	
		B22	Upper bathyal sediment (0–1 cm)	545	27.29	71.05	02–29/11/2010	
		B07	Lower bathyal sediment (0–1 cm)	920	25.07	70.66	02–29/11/2010	
		B05	Lower bathyal sediment (0–1 cm)	957	27.5	71.13	02–29/11/2010	
		B11	Lower bathyal sediment (0–1 cm)	1,113	23.85	70.65	02–29/11/2010	
		B04	Lower bathyal sediment (0–1 cm)	1,200	27.45	71.16	02–29/11/2010	

vehicle (Lander "Audacia") equipped with 2 10L-Niskin bottles (Table 1). SBE43 oxygen sensors were installed on the rosette's CTD and on the hadal Aanderaa optode sensor for the Audacia Lander. We sieved between ~0.5 and 60 L of seawater through a 20 μm nylon mesh and then gently filtered sampled onto pre-combusted (450º C, 24 hr) Whatman GFFs filters (0.7 μm nominal pore size) using pressurized canisters for bulk elemental and stable isotope analysis. Filters were immediately dried at 60ºC for 24 hr and kept dry in the dark until their analysis in the laboratory.

Bathyal and hadal sediment samples were obtained during the German RV *Sonne* cruises SO211 (ChiMeBo, 2–29 November 2010; Matys et al., 2017) and SO261, respectively (Figure 1). Samples were collected using a multi-corer (MUC; Barnett et al., 1984) equipped with 12 60 cm-long acrylic tubes (6–10 cm diameter for bathyal sediments and 9.5 cm diameter for hadal sediments). We used nine hadal surface (0–1 cm) and subsurface (1–2 and 2–3 cm) sediments (three sites between 7,734 and 8,063 m); these three depths were analyzed independently. In addition to seven bathyal surface sediments (seven sites between 529 and 1,200 m) for bulk elemental and stable isotope analysis (Table 1). We then compare our results with published data on sediment trap material for the region overlying the Atacama Trench (e.g., González et al., 2004; Hebbeln, Marchant, & Wefer, 2000).

2.2. Bulk Elemental and Stable Isotope Analysis of Carbon and Nitrogen

Particulate organic carbon (POC) and particulate organic nitrogen (PON), as well as their respective bulk stable isotopes (δ^{13}_{POC} and $\delta^{15}N_{PON}$) were measured in the Laboratory of Biogeochemistry and Applied Stable Isotopes at the Pontifical Catholic University of Chile. Prior to analysis, inorganic carbonates were removed by acidification of samples overnight with HCl fumes. Filters were then packed into tin capsules and fed via flash combustion (1,020ºC) into a Thermo Scientific Flash 2000 CHN elemental analyzer (EA) coupled to a Thermo DeltaV Advantage isotope ratio mass spectrometer (IRMS). Isotope ratios are reported using the standard (δ) notation and expressed as per mil (‰) with respect to standard reference material:

$$\delta X\ (‰) = \left[(R\text{sample} / R\text{standard}) - 1\right] * 1,000 \quad (1)$$

Where X is the $^{13}C_{POC}$ or $^{15}N_{PON}$, R is the corresponding ratio of $^{13}C/^{12}C$ or $^{15}N/^{14}N$ in a sample or standard (PDB for carbon and atmospheric N_2 for nitrogen). Analytical precision was calculated as ±0.215% and ±0.33% for nitrogen and carbon, respectively, based on four standards run in triplicate (acetanilide, atropine, caffeine, and glutamic acid). The analytical precision in the elemental analysis was ±0.003 and ±0.007 mg for nitrogen and carbon, respectively. The standard used for this calculation was Acetanilide (71.10% C and 10.36% N).

Sediment samples were analyzed using a Thermo Scientific EA—Delta V IRMS at the CU Boulder Earth Systems Stable Isotope Laboratory. Purified acetanilide and ethylenediaminetetraacetic acid were measured as standards for external calibration and drift corrections. The analytical precision for total organic carbon and total nitrogen was ±0.2% and ±0.11%, respectively, whereas the analytical precision was ±0.2‰ and ±0.15‰ for $\delta^{13}C_{POC}$ and $^{15}N_{PON}$, respectively.

2.3. Satellite POC Estimates

We used the mean and standard deviation (±STD) from satellite POC (POCsat) data for a ~90-days period (January-March 2018) prior to in situ POC sampling during the HADES expedition (March 2018) to evaluate the dynamics of POC in surface (0 m) and subsurface (1,000 m) waters over the Atacama Trench (Figures 6a–6d). Our reasoning assumes that particles found at 1,000 m must have originated in surface waters within that time. Additionally, POCsat values were averaged and binned into years for a 24-year period (1998–2022) to evaluate the seasonal (Figure S1 in Supporting Information S1) and annual variability in this region (Figure S2 in Supporting Information S1). POCsat was obtained from Copernicus Marine Service Information (https://marine.copernicus.eu/es) (MULTIOBS_GLO_BIO_BGC_3D_REP_015_010). This product merges satellite ocean color and Argo data using a neural network-based method and has shown strong potential to infer the global-scale vertical distribution of bio-optical properties with high space-time resolution, 0.25° × 0.25° horizontal resolution, and over 36 depth levels from the surface to 1,000 m (Sauzède et al., 2016).

2.4. Particle Flux Parameterization

We used empirical models to estimate vertical POC export fluxes from the surface to hadalpelagic depths. The most common model is the normalized power function known as the "Martin Curve" (Martin et al., 1987), which

equates the POC flux $f_p(z)$ [mg m^{-2} d^{-1}] at any depth z [m] with the export flux (C) at the reference depth, that is, at the base of the euphotic zone (Ez) according to Buesseler et al. (2020):

$$f_p(z) := C(z/Ez)^{-b} \quad (2)$$

The Ez was assumed to be 85 m (from 63 to 118 m depth) as reported by Pizarro et al. (2002) for this region. The b is the attenuation coefficient, which depends on the balance between POC sinking speed w [m day^{-1}] and the rate of remineralization k [1 day^{-1}] (Middelburg, 2019). The b value suggested for the open Pacific Ocean is 0.858 (Martin et al., 1987), whereas similar values have been suggested by open ocean waters off Antofagasta (0.834; González et al., 2009). However, lower b values (0.319) have also been suggested for the Peru region and the eastern tropical North Pacific due to the impact of oxygen deficiency on particle export (Van Mooy et al., 2002). In this study, we used a range of b values (0.36–1.33, average of = 0.78, n = 13) to calculate flux attenuation following Fernández-Urruzola et al. (2021). Given the inherent uncertainties of biogeochemical models, we tested a series of parameterizations, such as the basic exponential model (Banse, 1990), the original depth-attenuation rational model (Suess, 1980), and the double exponential model (Lutz et al., 2002) to estimate a range of POC flux values reaching hadal depths (Figure 7a, Table S1). We then compared these estimates to published POC fluxes in the region derived from moored sediment traps (González et al., 2004; Hebbeln, Marchant, & Wefer, 2000), free-drifting sediment traps (Wakeham et al., 1984), and particulate ^{230}Th-normalized isotope-based samples (Pavia et al., 2019) (Figure 7a, Table S1 in Supporting Information S1).

2.5. Statistical Analyses

We used averages and standard deviation for displaying the POCsat, and linear regressions to reveal significant correlations between theoretical models of vertical POC export fluxes and the available data derived from the sediment traps ($p < 0.001$). Statistical differences to $^{13}C_{POC}$ or $\delta^{15}N_{PON}$ in each environment were identified by ANOVA and Tukey's HSD (honestly significant difference) post hoc test. We used the MixSIAR (Version 3.2.0) mixing model to calculate the contribution of different OM sources according to Stock et al. (2018). Statistical tests were calculated using the vegan package (Oksanen et al., 2013) of the open-source software *R* version 3.6.2 with the ggplots package (Warnes et al., 2015).

3. Results

3.1. Elemental and Stable Isotope POM Signatures From Surface to Hadalpelagic Waters

The water column dissolved oxygen profile displays its lowest values within the oxygen-deficient zone (ODZ, 60–500 m depth), which coincides with low $\delta^{13}C_{POC}$ and $\delta^{15}N_{PON}$ values and low C:N ratio values (Figures 2a–2d). The $\delta^{13}C_{POC}$ values in the epipelagic zone showed a relatively large range, from −29.2‰ to −20.5‰ (mean −26.05‰ ± 1.8‰, n = 13, Figure 3a), and were statistically different from those in the ODZ (Tukey HSD post hoc test, $p < 0.05$, Figure 3c). The differences in the $\delta^{13}C_{POC}$ values between the epipelagic and the deeper oxygenated layers, on the contrary, were not statistically significant ($p > 0.05$; Figure 3c). The POC was isotopically enriched in ^{13}C at 5,000 m (−25.4‰ at sites A2 and A4, and −21.6‰ at site 6) compared to other depths (see Figure 2b).

The $\delta^{15}N_{PON}$ values ranged between 5.4 and 11.2‰ throughout the water column (mean 8.41 ± 1.37‰) (Figure 2c) and showed a statistical difference ($p < 0.05$) between the epipelagic zone and the deeper layers (i.e., mesopelagic, bathypelagic, abyssopelagic, and hadalpelagic zone) (see Figure 3d). Overall, the $\delta^{15}N_{PON}$ values decreased with increasing water depth down to 5,000 m, with values of 9.4, 8.4, and 7.4‰ at sites A2, A4, and A6, respectively. Below 5,000 m, however, $\delta^{15}N_{PON}$ increased at sites A2 and A6. This pattern was the opposite at site A4, where $\delta^{15}N_{PON}$ reached the lowest value (5.4‰) in the pelagic zone (Figure 2c).

The C:N ratio varied between 7.0 and 23.6 (mean value of 11.2 ± 3.2, Figure 2d) throughout the water column. Despite this large overall range, we found a lack of significant difference ($p > 0.05$) between depth layers (Figure 3e). Generally, the C:N ratios showed a consistent pattern between sites A2, A4, and A6. A high variability at the surface, a tendency to decrease toward 5,000 m, and then a slight increase toward 8,000 m (Figure 2d).

3.2. Differences in Elemental and Stable Isotope Signatures Between Bathyal and Hadal Sediments

In hadal and bathyal sediments, $\delta^{13}C_{POC}$ ranged from −23.6 to −22.7‰ (mean −23.2 ± 0.3‰) and from −22.9 to −21.8‰ (mean −22.2 ± 0.4‰), respectively (see Figures 4a and 4b). The range of $\delta^{15}N_{PON}$ values in hadal

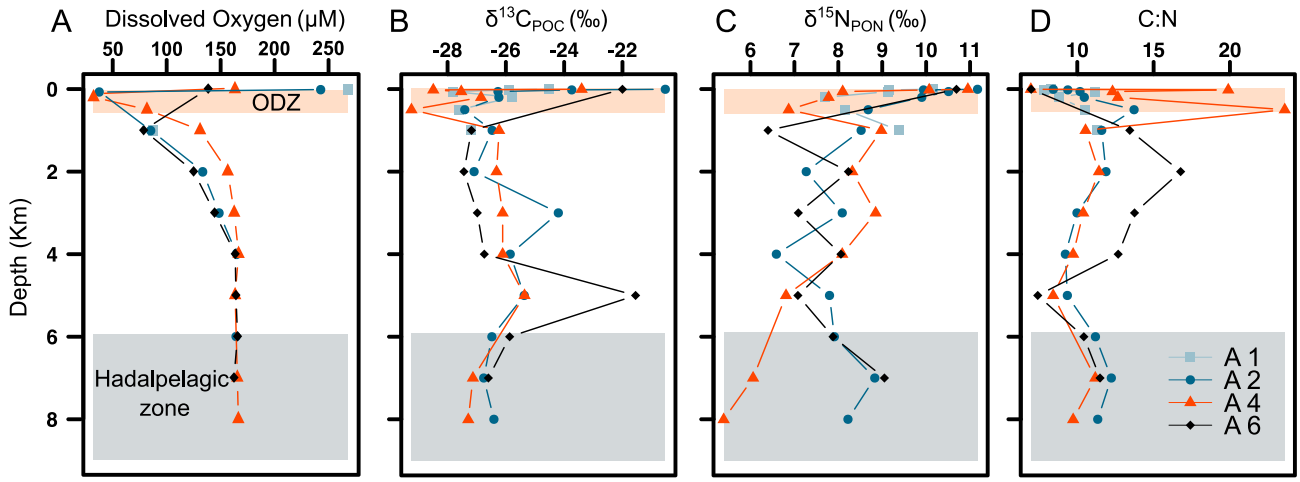

Figure 2. Water column depth profiles of (a) Dissolved oxygen, (b) $\delta^{13}C_{POC}$ (c) $\delta^{15}N_{PON}$, and (d) C:N ratio over the Atacama Trench. The orange and gray areas represent the oxygen deficient zone (ODZ; 60–500 m depth) and pelagic hadal zone (>6,000 m depth), respectively.

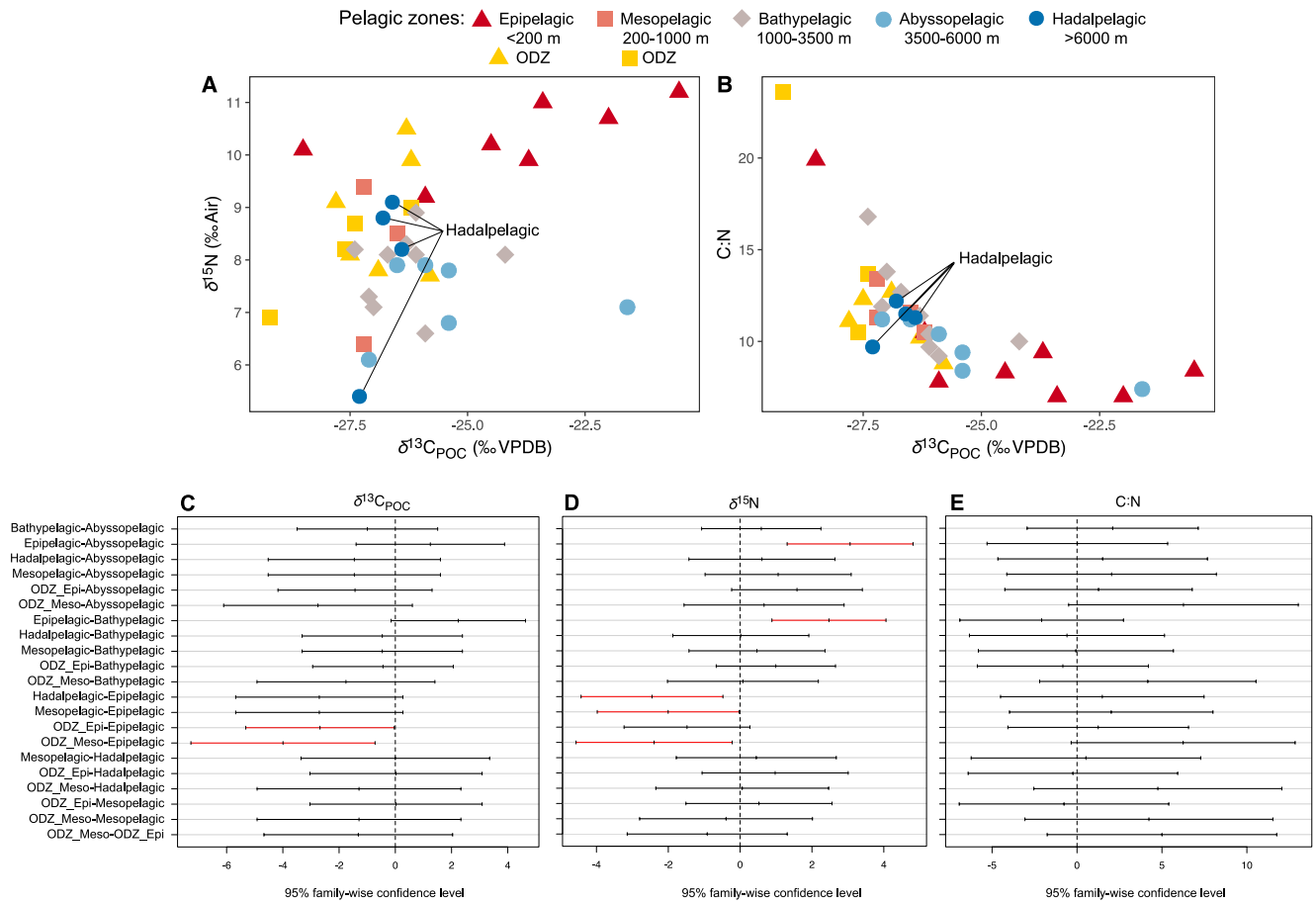

Figure 3. Biplots of (a) $\delta^{13}C_{POC}$ and $\delta^{15}N_{PON}$ and of particulate organic matter, and (b) $\delta^{13}C_{POC}$ and C:N ratios. The water column was divided by depth regions into the epipelagic (<200 m), mesopelagic (200–1,000 m), bathypelagic (3,500–6,000 m), and hadalpelagic (>6,000 m) zones. Panels C, D and E describe the 95% family-wise confidence intervals for the differences in the mean values of $\delta^{13}C_{POC}$, $\delta^{15}N_{PON}$ and C:N, respectively. Red lines indicate the occurrence of statistically significant differences (pairwise comparison by Tukey's test, $p < 0.05$).

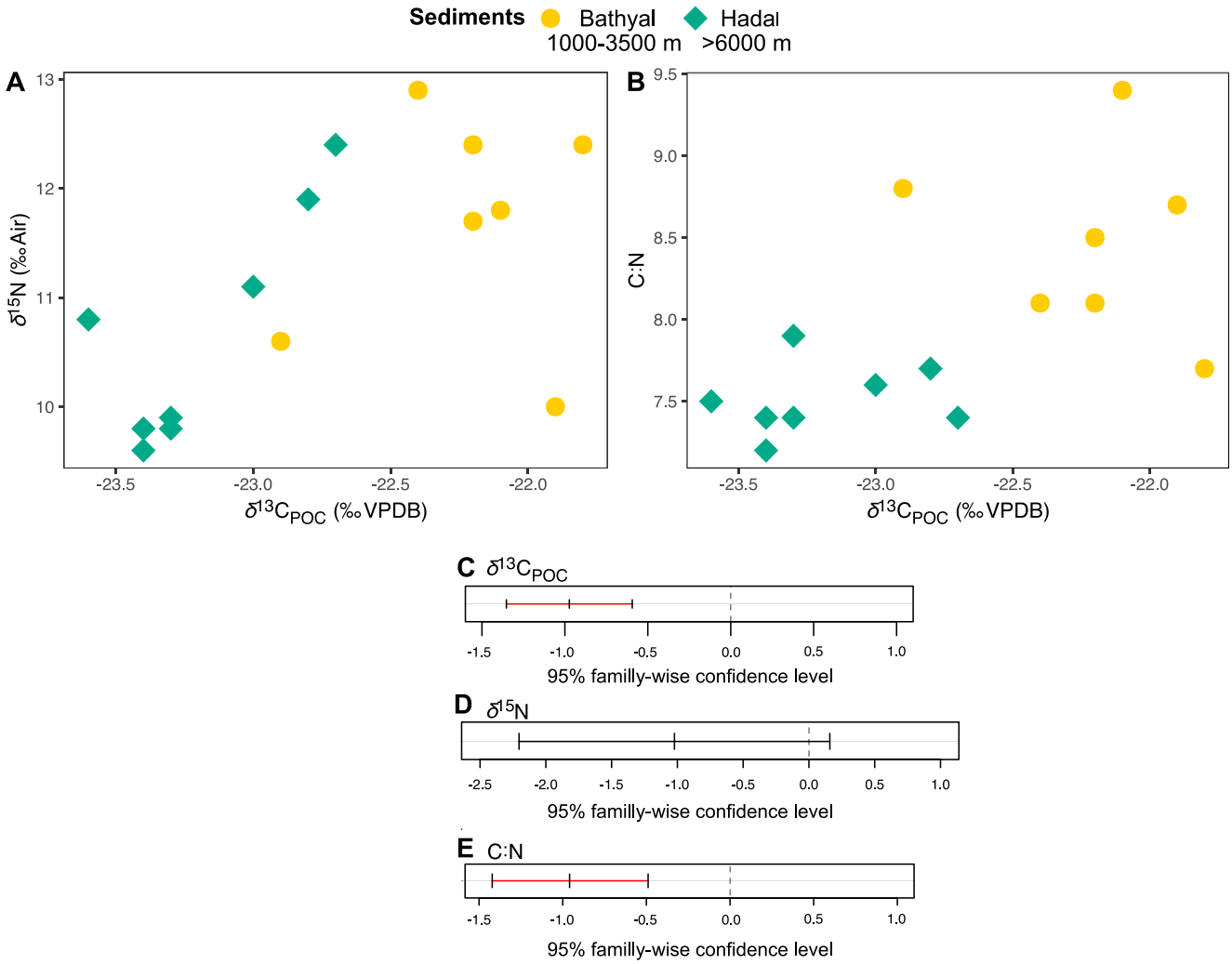

Figure 4. Biplots showing the relationship between (a) $\delta^{13}C_{POC}$ and $\delta^{15}N_{PON}$, and (b) $\delta^{13}C_{POC}$ and C:N ratios in bathyal and hadal sediments. Plots C, D, and E show the 95% family-wise confidence intervals of the difference between $\delta^{13}C_{POC}$, $\delta^{15}N_{PON}$, and C:N ratios, respectively. The red line indicates means that are significantly different with pairwise comparison by Tukey's test.

and bathyal sediments was 9.6–12.4‰ (mean 10.7 ± 1.1‰) and 10.0–12.9‰ (mean 11.7 ± 1.0‰), respectively (Figure 4a). The C:N ratio values were more homogeneous and significantly lower in hadal sediments (7.5 ± 0.2) compared to those found in bathyal sediments (8.5 ± 0.6) (Figure 4b). A Tukey HSD post hoc test revealed statistical differences in the $\delta^{13}C_{POC}$ values ($p < 0.001$) and C:N ratios ($p < 0.05$) between bathyal and hadal surface sediments. On the contrary, we found no significant differences in the $\delta^{15}N_{PON}$ values (see Figures 4c–4e).

3.3. Differences in Elemental and Stable Isotope Signatures Between the Water Column and Trench Sediments

We found that the $\delta^{13}C_{POC}$, $\delta^{15}N_{PON}$, and C:N values from the water column and bathyal and hadal surface sediments were statistically different among themselves (Box plots and Tukey's HSD post hoc test, $p < 0.05$, Figure 5). Thus, the largely overlapping pelagic values tended to be more depleted in ^{13}C and ^{15}N compared to bathyal and hadal surface sediments (Figures 5a and 5b). The C:N ratio displayed lower values in hadal and bathyal surface sediments than in the pelagic zone (Figure 5c).

3.4. POCsat in the Water Column Overlying the Atacama Trench

POCsat between 18° and 30°S showed high variability during the summer of 2018, ranging ~50–110 (±30 mg C m^{-3}) in surface waters and ~15–30 (±3 mg C m^{-3}) in subsurface waters (1,000 m) (Figure 6).

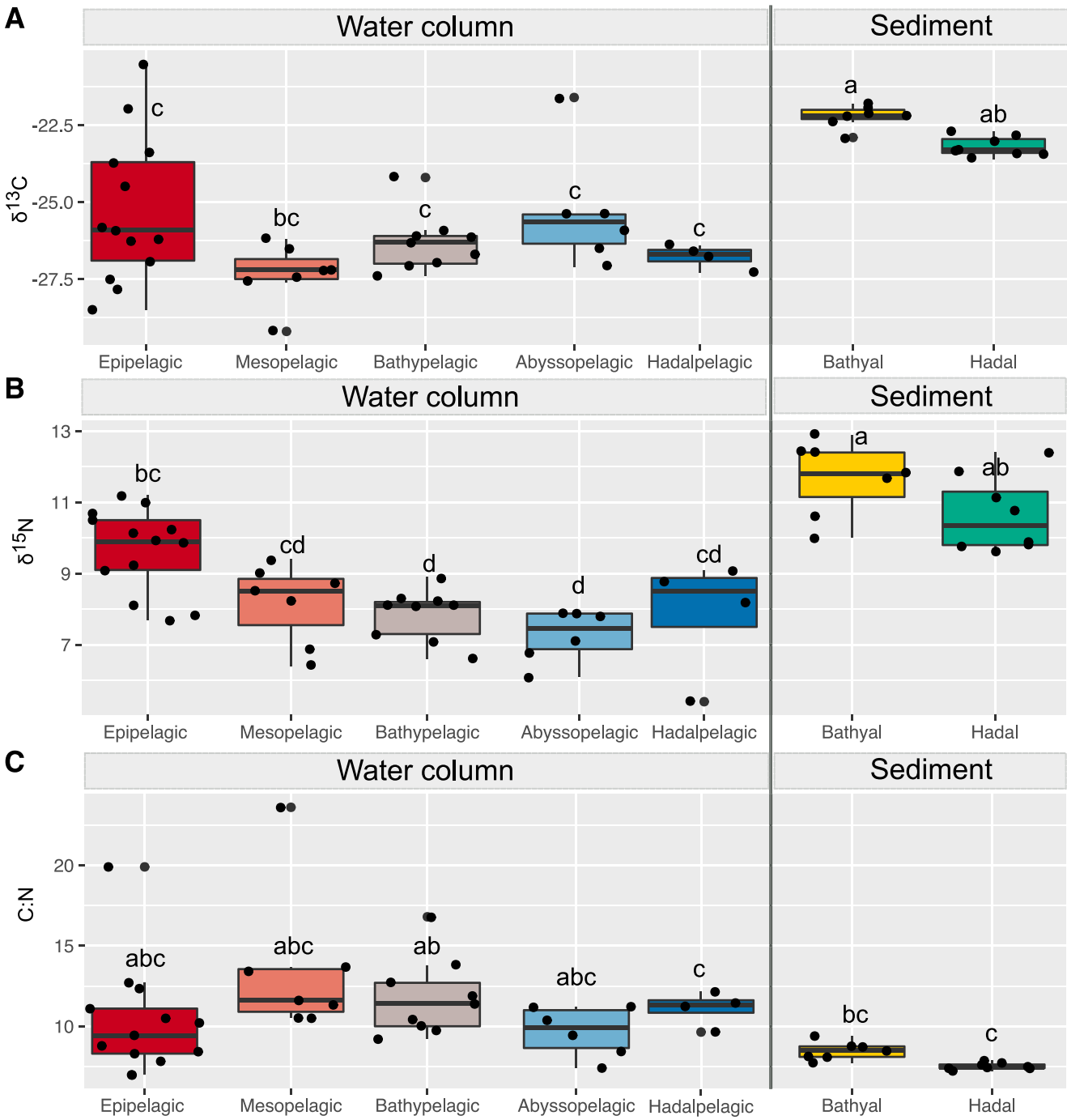

Figure 5. Boxplot showing the (a) $\delta^{13}C$, (b) $\delta^{15}N$, and (c) C:N values of the different depth regions of the water column and the bathyal and hadal sediments. We use the same depth zonation as in Figure 3. The letters used serve the purpose of indicating whether there are statistically significant differences among the compared groups. Groups that share the same letter do not show statistically significant differences, while groups with different letters indicate significant differences ($p < 0.05$, Tukey's test).

The overall POCsat decrease throughout the upper 1,000 m of the water column was ~73–84% (Figures 6a and 6c). The POC concentrations in surface and subsurface waters increased consistently southwards, especially between 28 and 30°S (Figures 6a and 6c), peaking right above the deepest area of the Atacama Trench with surface values up to ~110 ± 30 mg C m^{-3} (Figures 6a and 6b). In surface waters of the northernmost region (~18°S–26°S), we observed higher monthly average POC values in winter (~80–90 ± 10 mg C m^{-3}) and spring (~90–110 ± 12 mg C m^{-3}) than in summer and autumn (~60–70 ± 7 mg C m^{-3}) (Figure S1 in Supporting

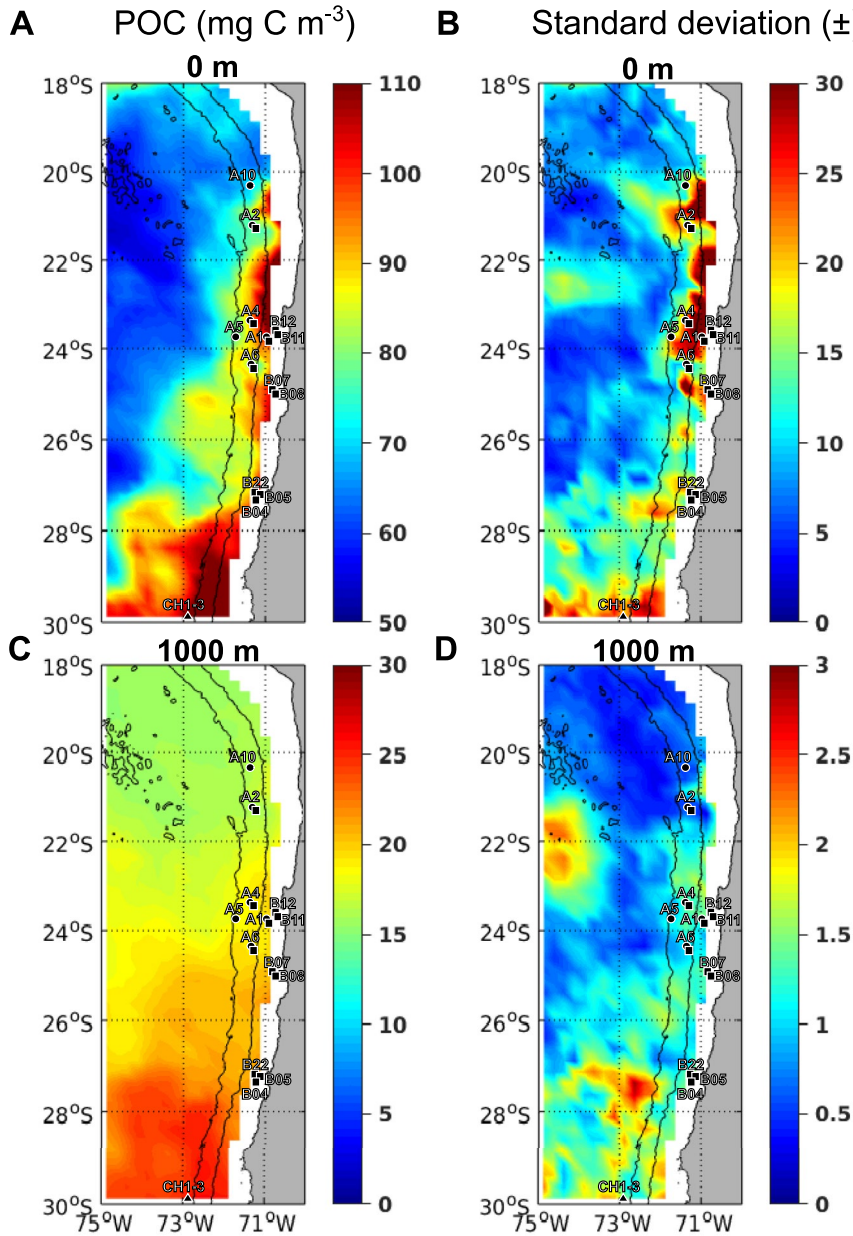

Figure 6. (a), (c) Spatial-temporal variability of POCsat calculated for mean weekly observations ~90 days prior to the Hades expedition (January-March 2018) in surface (0 m) and subsurface (1,000 m) waters, and (b and d) their respective ± standard deviations.

Information S1). However, between 28°S and 30°S, the summer POC concentrations were as high as in spring, although more variable. These trends were similar in the more stable subsurface waters, where the highest POC values were observed in summer between 24°S and 30°S (Figure S1 in Supporting Information S1).

3.5. Modeled Versus Observed POC Fluxes

Model calculations that include a lower attenuation of POC flux in the upper part of the photic zone (i.e., exponential curve from Banse, 1990; depth-attenuation rational from Suess, 1980; and double exponential from Lutz et al., 2002) result in fluxes that decline dramatically from ~120 mg C m^{-2} d^{-1} in surface waters to ~1 mg C m^{-2} d^{-1} at 1,000 m depth (Figure 7a). With this configuration, depth-attenuation rational and double exponential models display an enhanced fit (adjusted $R^2 = 0.6$) with mesopelagic and upper bathypelagic POC

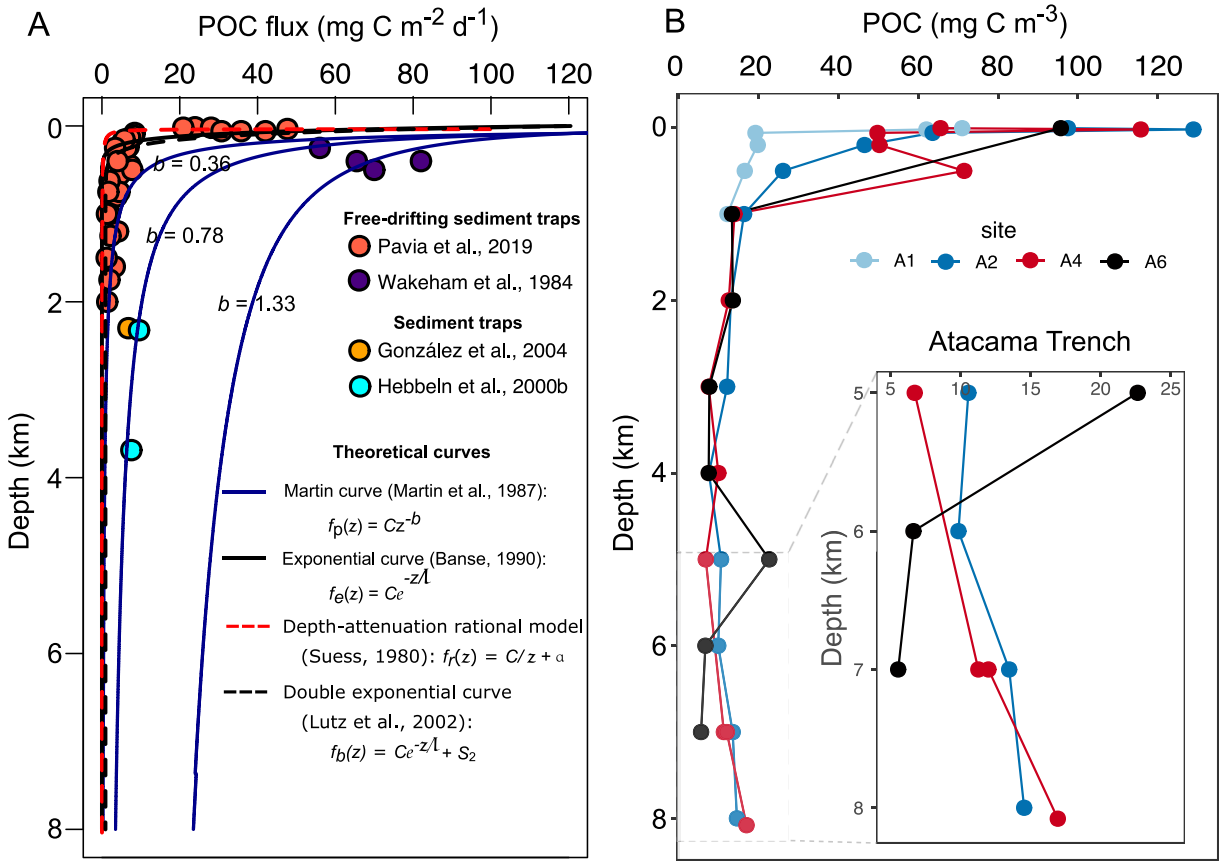

Figure 7. Particulate organic carbon (POC) fluxes and concentrations in the water column overlying the Atacama Trench (a) Empirical estimates of POC fluxes (mg C m^{-2} d^{-1}) obtained from (i) the Martin curve using 0.36, 0.78, and 1.33 as attenuation coefficients (blue lines), (ii) an exponential curve (black line), (iii) depth-attenuation rational (red dashed line), and (iv) double exponential curve (black dashed line). Solid circles indicate measured POC fluxes from deep-moored sediment traps (González et al., 2004; Hebbeln, Marchant, & Wefer, 2000), free-drifting sediment traps (Wakeham et al., 1984), and ^{230}Th-normalized isotope-based samples (Pavia et al., 2019). (b) In situ POC concentrations measured at stations A2, A4, and A6 during the Hades expedition. The inset highlights the depth region between 5,000 and 8,000 m.

fluxes (<2,000 m depth) derived from ^{230}Th off the coast of Peru (Pavia et al., 2019). The power-law model (Martin et al., 1987), on the other hand, displays an increase in the magnitude of POC fluxes, even though the attenuation is higher, concomitant with an increase in the attenuation coefficient. The average attenuation coefficient (b = 0.78) shows the best fit with the power-law model of POC fluxes measured from sediment traps at 2,300 m and 3,700 m depth in this region (González et al., 2004; Hebbeln, Marchant, & Wefer, 2000) (Figure 7a).

On the other hand, in situ POC concentrations (Figure 7b) decreased from ∼120 to ∼16.33 mg C m^{-3} in the top 1,000 m of the water column, which represents a degradation of 83.67%. Despite this trend, we observed an increase in the POC concentration up to 22.64 mg C m^{-3} at 5,000 m followed by a decline to 5.55 mg C m^{-3} at 8,000 m at site A6 (see inside panel in Figure 7b). Additionally, we observed a slight increase from 5,000 m at sites A2 (10.6 mg C m^{-3}) and A4 (6.7 mg C m^{-3}) to 8,000 m (14.5 and 16.9 mg C m^{-3}, respectively) (see inside panel in Figure 6b).

4. Discussion

4.1. Organic Matter Provenance

The stable carbon and nitrogen isotope signatures of phytoplankton, which constitute most of the OM (>80% of OM) produced in the euphotic zone (Lee et al., 2004), are influenced by: (a) the isotopic composition of the source carbon and nitrogen, (b) isotopic fractionation during carbon fixation and nutrient assimilation, and (c) isotopic fractionation during catabolic processes (Goericke & Fry, 1994). Thus, several processes can impact

the isotopic composition of carbon and nitrogen in surface waters, and consequently, the isotopic signature of bulk OM. These include the upwelling of subsurface waters, fluvial input, trophic interactions, and ecological successions (Peterson & Fry, 1987, and references therein), which are all dynamic in the euphotic zone. Our results show a large range in $\delta^{13}C_{POC}$ (−28.5 to −20.5‰, mean −25.30‰ ± 2.36) and $\delta^{15}N_{PON}$ (7.7–11.2‰, mean 9.64‰ ± 1.18) in the epipelagic zone (Figures 2a and 2b and 3). These values are within the range of those previously reported in surface POM in the Atacama region (Barrios-Guzmán et al., 2019), and consistent with a predominantly marine planktonic origin (Williams & Gordon, 1970). We anticipate that POM from the ODZ influences the lower epipelagic and upper mesopelagic zones, where the POM is isotopically depleted in ^{13}C and ^{15}N compared to shallower depths (Figures 2a, b, and 3a). It is important to emphasize that during the remineralization of OM, microorganisms require a balanced C:N ratio for growth, and there may be relatively high amounts of carbon relative to nitrogen in the by-products resulting from preferential nitrogen decomposition (Cavan et al., 2017). Similarly, fermentation, as an anaerobic metabolic process, involves the breakdown of carbohydrates into simpler compounds such as organic acids, alcohol, and other substances. During this process, microorganisms may exhibit a preference for utilizing the carbon found in carbohydrates over the available nitrogen. This preference can result in a higher C:N ratio in the fermentation products (Srain et al., 2020). Collectively, these processes contribute to an elevated C:N ratio in POM (Cavan et al., 2017; Srain et al., 2020).

Conversely, microbial respiration and biological oxidation, characterized by their preferential consumption of carbon and subsequent release of CO_2 during microbial metabolism, lead to a decrease in the relative content of organic carbon compared to organic nitrogen, ultimately reducing the C:N ratio of POM (Kong et al., 2021).

In fact, the observed isotopic depletion in $\delta^{13}C_{POC}$ values can be attributed to the contribution of biomass from dark autotrophic carbon fixation by chemolithoautotrophs in the ODZ waters (Callbeck et al., 2018; Ruiz-Fernández et al., 2020; Vargas et al., 2021). Moreover, in this environment, widespread microbial denitrification along the ETSP (De Pol-Holz et al., 2009) results in a reduction of bioavailable nitrogen, causing a nitrogen imbalance compared to carbon. Overall, this nitrogen imbalance likely contributes to the significant differences observed in the C:N ratio, particularly within the ODZ (Figure 2d).

It is important to note that the epipelagic zone (<200 m) exhibits distinctly marine phytoplankton geochemical signals a low C:N ratio and high $\delta^{13}C_{POC}$ values (Codispoti & Christensen, 1985; Goericke & Fry, 1994). In contrast, the ODZ is characterized by a high C:N ratio and low $\delta^{13}C_{POC}$ values, suggesting the dominance of chemoautotrophic microbial processes (Vargas et al., 2021). While we cannot completely rule out the possibility that high C:N and low $\delta^{13}C_{POC}$ values in the water column inside and around the ODZ may have a terrestrial origin (e.g., Valdés et al., 2004), this is unlikely given the low vegetation coverage in the continental region around the Atacama desert in addition to the absence of rivers in the area (see Figure 3b, Figure S4 in Supporting Information S1).

The bathypelagic zone displayed $\delta^{13}C_{POC}$ values between −27.4 and −24.2‰ (mean −26.31‰ ± 0.94, $n = 9$) and $\delta^{15}N_{PON}$ values between 6.6 and 8.9‰ (mean 7.85‰ ± 0.7), whereas the abyssopelagic zone displayed similar values for $\delta^{13}C_{POC}$ between −27.1‰ and −25.4‰ (mean −26.06‰ ± 0.73, $n = 6$) and for $\delta^{15}N_{PON}$ between 6.1 and 7.9‰ (mean 7.3‰ ± 0.81) (Figures 2a and 2b and 3a). However, compared to all other stations in the abyssopelagic zone, we detected ^{13}C-enriched POC at 5,000 m in station A6 (−21.6‰). This ^{13}C enrichment was associated with a decrease in the C:N ratio (7.4) (Figure 2b, d) and a slight increase in POC concentration (~22 mg C m^{-3}) (Figure 7b), but with no change in $\delta^{15}N_{PON}$ values (Figure 2c). Whereas this ^{13}C enrichment at 5,000 m in station A6 is atypical for deep waters, it is in the range of values observed in the epipelagic zone. Since the $\delta^{13}C$ of POM is relatively uniform in the deep-sea (Follett et al., 2014; Menzel & Ryther, 1968), it is unlikely that the observed ^{13}C enrichment in POM originates from in situ heterotrophic metabolism, as it would have the opposite effect, namely a more negative signature. Therefore, it is possible that the POM at this depth could be influenced by an epipelagic source, supported by the fast-sinking particle mechanism proposed by Fernández-Urruzola et al. (2021) for this region. However, we cannot rule out other mechanisms such as the resuspension of particles through downslope sediment transport or deep nepheloid layers.

The hadalpelagic zone displays a narrow range of $\delta^{13}C_{POC}$ values (from −27.3 to −26.4‰, mean −26.7‰ ± 0.38, $n = 4$), and a high range in $\delta^{15}N_{PON}$ (from 5.4 to 9.1‰, mean 7.87‰ ± 1.69) (shaded area in Figures 2a and 2b; and Figures 5a and 5b). Overall, the increase in $\delta^{15}N_{PON}$ values in the hadalpelagic zone coincides with an increase in the C:N ratio. This could indicate preferential nitrogen degradation with its resulting isotopic enrichment (Figures 2a–2c). This degradation appears to have a small impact on C isotopes, which show a lower effect

of isotopic composition compared to N and show less variation or sensitivity to changes in isotopic composition with respect to their origin as suggested by Rafter et al. (2019) for non-hadal depths. Furthermore, we speculate that sediment resuspension within the Atacama Trench could modestly contribute to the release of sedimentary OM into the deeper hadalpelagic zone. Nonetheless, it should be noted that this slight increase is not substantial enough to indicate a significant role in resuspension (Figure 7b). However, the limited spatial and temporal resolution of our hadalpelagic data set prevents us from contrasting these isotopic signatures at length.

Hadal surface sediments displayed a narrow range of $\delta^{13}C_{POC}$ (from −23.6‰ to −22.7‰, mean −23.18‰ ± 0.31, $n = 9$) and C:N ratios (from 7.2 to 7.9, mean 7.5 ± 0.21), and a wide range in $\delta^{15}N_{PON}$ (from: 9.6–12.4‰, mean 10.66‰ ± 1.06) (Figures 5a–5c). Furthermore, bathyal surface sediments displayed a narrow range of $\delta^{13}C_{POC}$ (from −22.9 to −21.8‰, mean −22.21‰ ±0.36, $n = 7$), and a wide range of C:N values (from 7.7 to 9.4, mean 8.4 ± 0.56) and $\delta^{15}N_{PON}$ (from 10‰ to 12.9‰, mean 11.68‰ ± 1.04) (Figures 5a–5c). Despite the thousands of meters separating hadal and bathyal sediments, they exhibited small differences between their average isotopic ($\delta^{13}C_{POC}$ ~ −0.97‰; $\delta^{15}N_{PON}$ 0.9‰) and C:N ratio (1.02) averages. This similarity could be due to, (a) a similar POM origin; (b) downslope sediment transport from the bathyal to the hadal region; (c) the production of in situ biomass from organisms with metabolisms involving similar isotopic fractionation; (d) Post-depositional diagenesis can account for the subtle isotopic differences observed between bathyal and hadal sediments (Fenton & Ritz, 1988; Gearing et al., 1984; Liu et al., 2022; Meyers, 1994). We note that a previous study on the bulk elemental and isotopic signature of abyssal and bathyal surface sediments (Hebbeln, Marchant, Freudenthal, & Wefer, 2000) reported $\delta^{13}C_{POC}$ values ~3‰ more enriched compared to the bathyal and hadal sediments of this study (see Figure S3 in Supporting Information S1). Previous studies in the hadal realm suggest that the characteristic high pressures and low temperatures of this environment promote a higher carbon isotopic fractionation in heterotrophic piezophilic bacteria compared to shallower surface heterotrophic bacteria (Fang et al., 2006; Xu et al., 2018). These processes combined could partly explain why the hadal sediments are isotopically lighter in $\delta^{13}C$ and $\delta^{15}N$ than bathyal sediments. However, other modes of nutrition (e.g., chemoorganotrophs and/or chemolithoautotrophs) and their associated isotopic fractionations in these environments remain understudied.

The geochemical study of Luo et al. (2017) on Mariana Trench sediments concluded that marine algae is the primary OM source in this system, as reflected in bulk C:N and $\delta^{13}C$ values. This result is consistent with previous studies in the Japan and Atacama Trenches (Danovaro et al., 2003; Nakatsuka et al., 1997). However, deeply buried sediment between 122 and 533 cm below sediment surface, corresponding to a time span of 4–13 Kyr from the Atacama Trench indicates the occurrence of alternating phases of slow pelagic sedimentation and rapid mass-wasting events, which fuel microbial carbon turnover at remarkably high rates (Glud et al., 2013; Zabel et al., 2022). Thus, we expect that the remineralization by piezophilic bacteria in the hadal region of OM originated from primary production in the surface ocean and from downslope transport will alter the isotopic composition of sedimentary carbon and nitrogen (Xu et al., 2018, and references therein).

In summary, the wide range of $\delta^{13}C_{POC}$ and C:N values in the overall water column complicates the use of various local end-member to disentangle the sources of OM reaching the hadal region of the water column and the sediment (Figure S4 in Supporting Information S1). The observed discrepancies between the isotopic signatures of POM in bathypelagic sediment traps (2,300–3,700 m; Hebbeln, Marchant, & Wefer, 2000 and references therein) and POM in the water column remain puzzling. Whereas we provide some possible explanations, they remain to be confirmed by future investigations. First, our water column data represents a discrete snapshot in time, whereas the weighted mass flux in sediment traps could primarily reflect the period when OM production and export are at their peak. Second, these isotopic differences could also be attributed to the spatial heterogeneity of OM sources (e.g., phytoplankton groups), encompassing both onshore and offshore variations, as well as variations within different pelagic zones of the water column (refer to Figure S4 in Supporting Information S1). Despite these differences, hadal sediments of the Atacama Trench exhibit distinctive C:N and $\delta^{13}C_{POC}$ values, likely resulting from the mixing of OM from the pelagic region, downslope transport, and in situ sedimentary microbial activity (Figure S4 in Supporting Information S1).

Changes in the composition, activity, and physiological adaptation of the chemoautotrophic and heterotrophic in situ hadal benthic microbial community of the Atacama Trench emerge as a factor influencing the elemental and isotopic composition of sedimentary OM. For example, this could be driven by bacterial processes such as anammox leading to rapid nitrogen loss within a shallow layer of the sediment surface (Thamdrup et al., 2021). Other recent studies have also highlighted potential physiological adaptations of the benthic microbial community to the

high-pressure and low-temperature present in the hadal realm though cell membrane lipid composition (Flores et al., 2022; Tamby et al., 2023), whereas long-term selective forces, where co-existing taxa are more dissimilar and the phylogenetic turnover is greater than expected over the redox zone, lead to large community shifts over time (Schauberger et al., 2023). Together, changes in the chemical composition of benthic microbes as well as their metabolisms could alter the overall elemental and stable isotope composition of sedimentary OM.

4.2. What Is the Relative Contribution of Allochthonous OM Sources to Atacama Trench Sediments?

Marine trenches have been reported to receive diverse sources of OM (Glud et al., 2013; Luo et al., 2017; Xu et al., 2018). In general, intra- and inter-trench heterogeneity in the composition of the sedimentary OM, along with benthic hadal remineralization rates, have been ascribed to differences in regional surface ocean productivity (Glud et al., 2021; Jamieson, 2015; Luo et al., 2018; Wenzhöfer et al., 2016). Sinking particles are key transport mechanisms delivering carbon to the deep ocean where it can be stored and effectively removed from the modern carbon cycle (Williams & Giering, 2022). In fact, fresh phytodetrital material from surface waters has been observed in hadal regions (Danovaro et al., 2003; Guo et al., 2018). Since the Atacama Trench underlies highly productive waters, it is reasonable to presume that this hadal system is more prone to receive particles synthesized in surface waters compared to oligotrophic trenches. However, a recent study on sedimentary profiles of $^{210}Pb_{ex}$ and TOC in the Atacama Trench demonstrated no apparent relationship between the net primary productivity at the surface ocean and the carbon mass accumulation rate in sediment (Oguri et al., 2022). These observations suggest that depositional dynamics and local bathymetry are more important than how much OM is produced at the surface. However, high remineralization due to intense heterotrophic activity in sediments has also been demonstrated in the Atacama Trench (Glud et al., 2013, 2021). Therefore, although previous studies have suggested an important contribution of sedimentary OM from shallower depths (continental shelf to bathyal region) to the hadal benthic zone (Flores et al., 2022; Oguri et al., 2022; Zabel et al., 2022), the contribution of OM from the euphotic zone to the hadalpelagic zone could be more than expected before is quickly degraded in sediments.

We evaluated changes in surface primary productivity through available POCsat data and modeled POC fluxes in the Atacama Trench. POCsat exhibits high concentrations and a high degree of spatial heterogeneity in surface waters over the Atacama Trench region (Figure 6a). This trend is modulated by offshore waters, where the chlorophyll maximum occurs in winter (Yuras et al., 2005), and can be related to the propagation of mesoscale eddies that expand the area of high chlorophyll concentration beyond the coastal upwelling center (Correa-Ramirez et al., 2007). We observed similar patterns of seasonal increase in POCsat in autumn and winter in the study area (Figure S1 in Supporting Information S1). Moreover, POCsat data below the epipelagic zone shows more attenuated spatial heterogeneity, which is maintained up to the lower limit of the mesopelagic zone (~16%–27% POC; Figure 6c). Our discrete measurements at the same depth (~16.3% POC; Figure 7b) are consistent with the POCsat results. Similar POC percentages in the mesopelagic zone have been reported in other high-productivity systems, which has been attributed to the presence of ODZ waters that could reduce the decomposition rate of POC and increase its sink into deeper waters (Ma et al., 2021; Weber & Bianchi, 2020).

Discrete measurements of OM composition from bathypelagic to hadalpelagic zones are scarce. Since POC concentrations in bathypelagic and upper abyssopelagic zones (i.e., 1,000–5,000 m; Figure 7b) are low and stable, we speculate that this could reflect a well-mixed deep layer, such as previously suggested in the Izu–Ogasawara Trench (Kawagucci et al., 2018). However, the slight POC increase in the hadalpelagic zone at stations A2 and A4 (see Figure 7b) may derive from an additional POC input in this region. Potential sources include POC accumulation due to the resuspended sediment, or a lateral contribution through nepheloid layers from the shallower slope (Gardner et al., 2022; Nakatsuka et al., 1997; Xu et al., 2018). Studies in the open ocean and the Gulf of Mexico have found that areas of high surface eddy kinetic energy are often related to areas where nepheloid layers are common (Gardner et al., 2022). However, it is unknown whether nepheloid layer can reach hadal depths (6,000–11,000 m). To investigate whether the production of POC in the epipelagic and mesopelagic zones affects POC fluxes at greater depths, we compared vertical POC fluxes calculated from theoretical models (see model parameters in Table S1 in Supporting Information S1) against published, in situ POC flux measurements derived from sediment traps in the region (Figure 7a). The theoretical calculations that best fit deep sediment trap data suggest a low POC flux (3.96 mg C m^{-2} d^{-1}, ~3.3%, see Figure 7a) from the euphotic zone to surface sediments of the Atacama Trench.

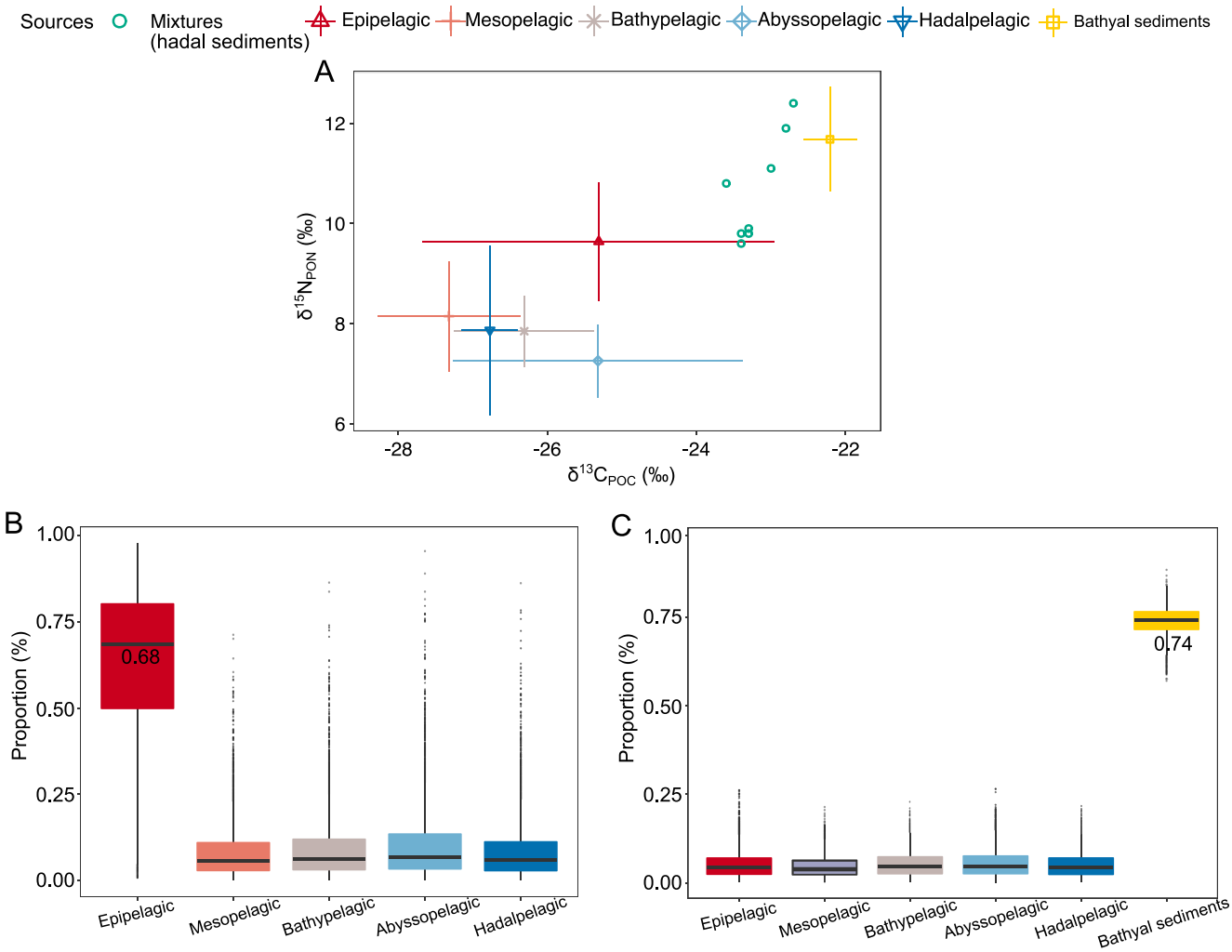

Figure 8. Isotopic signatures of organic matter and their mixing in surface hadal sediments (a) Biplot showing $\delta^{13}C$ and $\delta^{15}N$ of particulate organic matter (POM) in the water column and surface hadal sediments ("mixture"). (b) Biplot showing $\delta^{13}C$ and $\delta^{15}N$ of POM in the water column and surface hadal sediments ("mixture"), in addition to bathyal sediments as an additional source of POM. (c and d) Relative fractional contribution of POM from the different pelagic zones as well as from bathyal and hadal sediments using the MixSIAR (Stable Isotope Analysis in R) mixing model.

Given the multiple possible sources of OM to the deep ocean, we applied a multi-source percentage contribution model of Stock et al. (2018) to our isotope data set. When only pelagic OM sources are used, we observed that the epipelagic zone is the dominant (~68%) source of POM to hadal surface sediments (Figures 8a and 8b). However, when we include bathyal sediments as an additional source, the contribution to hadal sediments from the combined water column regions is <25% (Figures 8a and 8c). Thus, these results suggest that OM can rapidly reach the hadal zone, likely through a combination of fast-sinking particulates and downslope and/or lateral transport, as has been suggested in previous studies for the Atacama Trench (Fernández-Urruzola et al., 2021; Oguri et al., 2022; Zabel et al., 2022). We speculate that in addition to the processes described above, the slope of bathymetric relief ($\alpha = 6.5°$) in the Atacama trench (computed from GEBCO (2020) Grid; Kioka & Strasser, 2022), may be an additional factor contributing to sedimentary OM through downslope transport in this region.

We acknowledge that we cannot infer biogeochemical or microbial processes in the hadalpelagic zone by simply extrapolating POC fluxes from surface waters through isotope models without considering other allochthonous sources as well as autochthonous sources. Therefore, future studies should delve into the complexity of processes influencing POC flux models, such as sinking velocity (Williams & Giering, 2022) and the "source funnel" effect proposed by Sigel et al. (2008) and widely discussed by Fernández-Urruzola et al. (2021). Future measurements

of sediment trap fluxes from the bottom of the Atacama trench would allow us to quantify the contribution and composition of different OM sources, as well as understand its temporal variability.

5. Conclusions

We investigated the sources and mixing of OM in the hadal region of the Atacama trench using bulk elemental and stable isotope geochemical data. The $\delta^{13}C_{POC}$ and $\delta^{15}N_{PON}$ values in surface sediments of the Atacama Trench indicate the presence of a reservoir of isotopically heavier OM compared to the water column, albeit lighter than the bathyal sediments. Using a mixing model based on the isotopic signatures of bulk organic carbon and total nitrogen in pelagic POM and sedimentary OM, we calculated that ∼75% of the OM present in surface sediments from the Atacama Trench could derive from bathyal sediments. When bathyal sediment is excluded from the model, we computed that ∼68% of sedimentary OM in the hadal sediments could derive from the epipelagic region. Additionally, we report evidence of high spatial heterogeneity in surface water POC from remote-sensing data in the highly productive region overlying the Atacama Trench. Notably, the vertical POC fluxes that best fit with existing data from deep sediment traps (∼2,300 and 3,700 m) suggest that ∼3.3% of the total POC flux that reaches hadal surface sediments derives from surface waters. Thus, we conclude that the contribution from downslope sediment transport to the hadal benthic zone could be greater than the POM export from the water column. However, since the fluxes of these sources are expected to vary both spatially and temporally, and the fact that sediments integrate time scales larger than the water column, we cannot rule out a greater contribution from the surface epipelagic zones at times.

Data Availability Statement

Data from Hebbeln, Marchant, Freudenthal, and Wefer (2000), Hebbeln, Marchant, and Wefer (2000), González et al. (2004), and Wakeham et al. (1984) for sediments and sediment traps, along with supplementary data from Vargas et al. (2021) for the water column and Pavia et al. (2019) for surficial POC flux, were utilized to provide contextual information for this manuscript. POCsat was obtained from the Copernicus Marine Service Information (https://marine.copernicus.eu/es) (MULTIOBS_GLO_BIO_BGC_3D_REP_015_010), further details can be found in the methods section. The carbon and nitrogen isotopic signatures of the bulk organic matter for all samples in this study, as well as the corresponding R code, can be accessed through the following publication: Edgart (2023).

Acknowledgments
This work was supported by the Chilean National Agency for Research and Development through the Millennium Science Initiative-ANID Program (Grant ICN12 019N), grants FONDECYT 1191360 and 11221079 to O. Ulloa and I. Fernández-Urruzola, respectively, and by the European Research Council (HADES-ERC, Grant agreement number 669947 to R. Glud) and the Max Planck Society. J. Sepúlveda acknowledges partial support from NSF-CAREER award 2047057 and from the Department of Geological Sciences and INSTAAR at the University of Colorado Boulder. E. Flores was also partially supported by the Universidad de Concepción (UCO, 1866 student scholarship 2022). We are thankful to the captains, crews, and scientists of the German RV Sonne cruises SO261 (HADES-ERC) and SO211 (ChiMeBo). In particular, we thank the chief scientists R. Glud and F. Wenzhöfer (HADES-ERC) and Dierk Hebbeln (ChiMeBo), and Nadin Ramirez for the deployment of the Lander "Audacia" during the HADES-ERC cruise. The HADES-ERC and ChiMeBo cruises were funded by the European Research Council and the German Bundesministerium für Bildung and Forschung (BMBF), respectively. We thank Dr. Min Luo and an anonymous reviewer for their constructive comments that improved the quality and clarity of our manuscript.

References

Azam, F., Smith, D., Steward, G., & Hagström, Å. (1994). Bacteria-organic matter coupling and its significance for oceanic carbon cycling. *Microbial Ecology*, *28*(2), 167–179. https://doi.org/10.1007/BF00166806

Banse, K. (1990). New views on the degradation and disposition of organic particles as collected by sediment traps in the open sea. *Deep Sea Research Part A: Oceanographic Research Papers*, *37*(7), 1177–1195. https://doi.org/10.1016/0198-0149(90)90058-4

Barnett, P. R. O., Watson, J., & Connelly, D. (1984). A multiple corer for taking virtually undisturbed samples from shelf, bathyal and abyssal sediments. *Oceanologica Acta*, *7*(4), 399–408.

Barrios-Guzmán, C., Sepúlveda, M., Docmac, F., Zarate, P., Reyes, H., & Harrod, C. (2019). Sample acidification has a predictable effect on isotopic ratios of particulate organic matter along the Chilean coast. *Rapid Communications in Mass Spectrometry*, *33*(21), 1652–1659. https://doi.org/10.1002/rcm.8511

Bathymetric Compilation Group. (2020). *The GEBCO_2020 grid—a continuous terrain model of the global oceans and land*. British Oceanographic Data Centre, National Oceanography Centre, NERC.

Buesseler, K. O., Boyd, P. W., Black, E. E., & Siegel, D. A. (2020). Metrics that matter for assessing the ocean biological carbon pump. *Proceedings of the National Academy of Sciences*, *117*(18), 9679–9687. https://doi.org/10.1073/pnas.1918114117

Burd, A. B., & Jackson, G. A. (2009). Particle aggregation. *Annual Review of Marine Science*, *1*, 65–90. https://doi.org/10.1146/annurev.marine.010908.163904

Callbeck, C. M., Lavik, G., Ferdelman, T. G., Fuchs, B., Gruber-Vodicka, H. R., Hach, P. F., et al. (2018). Oxygen minimum zone cryptic sulfur cycling sustained by offshore transport of key sulfur oxidizing bacteria. *Nature Communications*, *9*(1), 1729. https://doi.org/10.1038/s41467-018-04041-x

Cantarero, S. I., Henríquez-Castillo, C., Dildar, N., Vargas, C. A., Von Dassow, P., Cornejo-D'Ottone, M., & Sepúlveda, J. (2020). Size-fractionated contribution of microbial biomass to suspended organic matter in the eastern Tropical South Pacific oxygen minimum zone. *Frontiers in Marine Science*, *7*, 540643. https://doi.org/10.3389/fmars.2020.540643

Cavan, E., Trimmer, M., Shelley, F., & Sanders, R. (2017). Remineralization of particulate organic carbon in an ocean oxygen minimum zone. *Nature Communications*, *8*(1), 14847. https://doi.org/10.1038/ncomms14847

Cavan, E. L., Kawaguchi, S., & Boyd, P. W. (2021). Implications for the mesopelagic microbial gardening hypothesis as determined by experimental fragmentation of Antarctic krill fecal pellets. *Ecology and Evolution*, *11*(2), 1023–1036. https://doi.org/10.1002/ece3.7119

Chunhui, X., Yonghong, W., Jiwei, T., Xuchen, W., & Yu, X. (2020). Mineral composition and geochemical characteristics of sinking particles in the Challenger Deep, Mariana Trench: Implications for provenance and sedimentary environment. *Deep Sea Research Part I: Oceanographic Research Papers*, *157*, 103211. https://doi.org/10.1016/j.dsr.2019.103211

Codispoti, L. A., & Christensen, J. P. (1985). Nitrification, denitrification and nitrous oxide cycling in the eastern tropical South Pacific Ocean. *Marine Chemistry*, *16*(4), 277–300. https://doi.org/10.1016/0304-4203(85)90051-9

Correa-Ramirez, M. A., Hormazábal, S., & Yuras, G. (2007). Mesoscale eddies and high chlorophyll concentrations off central Chile (29–39 S). *Geophysical Research Letters*, *34*(12), L12604. https://doi.org/10.1029/2007GL029541

Daneri, G., Dellarossa, V., Quiñones, R., Jacob, B., Montero, P., & Ulloa, O. (2000). Primary production and community respiration in the Humboldt Current System off Chile and associated oceanic areas. *Marine Ecology Progress Series*, *197*, 41–49. https://doi.org/10.3354/meps197041

Danovaro, R., Della Croce, N., Dell'Anno, A., & Pusceddu, A. (2003). A depocenter of organic matter at 7800 m depth in the SE Pacific Ocean. *Deep Sea Research Part I: Oceanographic Research Papers*, *50*(12), 1411–1420. https://doi.org/10.1016/j.dsr.2003.07.001

De La Rocha, C. L., Nowald, N., & Passow, U. (2008). Interactions between diatom aggregates, minerals, particulate organic carbon, and dissolved organic matter: Further implications for the ballast hypothesis. *Global Biogeochemical Cycles*, *22*(4). https://doi.org/10.1029/2007GB003156

de Melo Viríssimo, F., Martin, A. P., & Henson, S. A. (2022). Influence of seasonal variability in flux attenuation on global organic carbon fluxes and nutrient distributions. *Global Biogeochemical Cycles*, *36*(2), e2021GB007101. https://doi.org/10.1029/2021GB007101

De Pol-Holz, R., Robinson, R. S., Hebbeln, D., Sigman, D. M., & Ulloa, O. (2009). Controls on sedimentary nitrogen isotopes along the Chile margin. *Deep Sea Research Part II: Topical Studies in Oceanography*, *56*(16), 1042–1054.https://doi.org/10.1016/j.dsr2.2008.09.014

Devol, A. H., & Hartnett, H. E. (2001). Role of the oxygen-deficient zone in transfer of organic carbon to the deep ocean. *Limnology & Oceanography*, *7*, 1684–1690. https://doi.org/10.4319/lo.2001.46.7.1684

Edgart. (2023). *EdgartFlores/POC-Atacama-Trench (0.2.0)*. Zenodo. https://doi.org/10.5281/zenodo.7949351

Fang, J., Uhle, M., Billmark, K., Douglas, H., Bartlett, H., & Kato, C. (2006). Fractionation of carbon isotopes in biosynthesis of fatty acids by a piezophilic bacterium Moritella japonica strain DSK1. *Geochimica et Cosmochimica Acta*, *70*(7), 1753–1760. https://doi.org/10.1016/j.gca.2005.12.011

Fenton, G. E., & Ritz, D. A. (1988). Changes in carbon and hydrogen stable isotope ratios of macroalgae and seagrass during decomposition. *Estuarine, Coastal and Shelf Science*, *26*(4), 429–436. https://doi.org/10.1016/0272-7714(88)90023-6

Fernández-Urruzola, I., Ulloa, O., Glud, R. N., Pinkerton, M. H., Schneider, W., Wenzhöfer, F., & Escribano, R. (2021). Plankton respiration in the Atacama Trench region: Implications for particulate organic carbon flux into the hadal realm. *Limnology & Oceanography*, *66*(8), 3134–3148. https://doi.org/10.1002/lno.11866

Flores, E., Cantarero, S. I., Ruiz-Fernández, P., Dildar, N., Zabel, M., Ulloa, O., & Sepúlveda, J. (2022). Bacterial and eukaryotic intact polar lipids point to in situ production as a key source of labile organic matter in hadal surface sediment of the Atacama Trench. *Biogeosciences*, *19*(5), 1395–1420. https://doi.org/10.5194/bg-19-1395-2022

Follett, C. L., Repeta, D. J., Rothman, D. H., Xu, L., & Santinelli, C. (2014). Hidden cycle of dissolved organic carbon in the deep ocean. *Proceedings of the National Academy of Sciences*, *111*(47), 16706–16711. https://doi.org/10.1073/pnas.1407445111

Fuenzalida, R., Schneider, W., Garcés-Vargas, J., Bravo, L., & Lange, C. (2009). Vertical and horizontal extension of the oxygen minimum zone in the eastern South Pacific Ocean. *Deep Sea Research Part II: Topical Studies in Oceanography*, *56*(16), 992–1003. https://doi.org/10.1016/j.dsr2.2008.11.001

Gao, X., Yanga, Y., & Wang, C. (2012). Geochemistry of organic carbon and nitrogen in surface sediments of coastal Bohai Bay inferred from their ratios and stable isotopic signatures. *Marine Pollution Bulletin*, *64*(6), 1148–1155. https://doi.org/10.1016/j.marpolbul.2012.03.028

Gardner, W. D., Richardson, M. J., Mishonov, A. V., Bean, D. A., & Herguera, J. C. (2022). Nepheloid layers in the deep Gulf of Mexico. *Marine Geology*, *454*(December), 106950. https://doi.org/10.1016/j.margeo.2022.106950

Gearing, J., Gearing, P., Rudnick, D., Requejo, A., & Hutchins, M. (1984). Isotopic variability of organic carbon in a phytoplankton-based, temperate estuary. *Geochimica et Cosmochimica Acta*, *48*(5), 1089–1098. doi:. https://doi.org/10.1016/0016-7037(84)90199-6

Glud, R. N., Berg, P., Thamdrup, B., Larsen, M., Stewart, H. A., Jamieson, A. J., et al. (2021). Hadal trenches are dynamic hotspots for early diagenesis in the deep sea. *Communications Earth & Environment*, *2*(1), 1–8. doi:. https://doi.org/10.1038/s43247-020-00087-2

Glud, R. N., Wenzhöfer, F., Middelboe, M., Oguri, K., Turnewitsch, R., Canfield, D. E., & Kitazato, H. (2013). High rates of microbial carbon turnover in sediments in the deepest oceanic trench on Earth. *Nature Geoscience*, *6*(4), 284–288. https://doi.org/10.1038/ngeo1773

Goericke, R., & Fry, B. (1994). Variations of marine plankton δ13C with latitude, temperature, and dissolved CO2 in the world ocean. *Global Biogeochemical Cycles*, *8*(1), 85–90.https://doi.org/10.1029/93GB03272

González, H. E., Daneri, G., Iriarte, J. L., Yannicelli, B., Menschel, E., Barría, C., et al. (2009). Carbon fluxes within the epipelagic zone of the Humboldt Current System off Chile: The significance of euphausiids and diatoms as key functional groups for the biological pump. *Progress in Oceanography*, *83*(1–4), 217–227. https://doi.org/10.1016/j.pocean.2009.07.036

González, H. E., Hebbeln, D., Iriarte, J. L., & Marchant, M. (2004). Downward fluxes of faecal material and microplankton at 2300 m depth in the oceanic area off Coquimbo (30 S), Chile, during 1993–1995. Deep Sea Research Part II: Topical Studies in Oceanography, *51*(20–21), 2457–2474. [Dataset]. https://doi.org/10.1016/j.dsr2.2004.07.027

González, H. E., Ortiz, V., & Sobarzo, M. (2000). The role of faecal material in the particulate organic carbon flux in the northern Humboldt Current, Chile (23°S), before and during the 1997–98. *El Niño Journal of Plankton Research*, *22*(3), 499–529. https://doi.org/10.1093/plankt/22.3.499

Grabowski, E., Letelier, R. M., Laws, E. A., & Karl, D. M. (2019). Coupling carbon and energy fluxes in the North Pacific subtropical gyre. *Nature Communications*, *10*(1), 1–9. https://doi.org/10.1038/s41467-019-09772-z

Guo, R., Liang, Y., Xin, Y., Wang, L., Mou, S., Cao, C., et al. (2018). Insight into the Pico- and nano-phytoplankton communities in the deepest biosphere, the Mariana Trench. *Frontiers in Microbiology*, *9*, 2289. https://doi.org/10.3389/fmicb.2018.02289

Hebbeln, D., Marchant, M., Freudenthal, T., & Wefer, G. (2000). Surface sediment distribution along the Chilean continental slope related to upwelling and productivity [Dataset]. Marine Geology, *164*(3–4), 119–137. https://doi.org/10.1016/S0025-3227(99)00129-2

Hebbeln, D., Marchant, M., & Wefer, G. (2000). Seasonal variations of the particle flux in the Peru-Chile current at 30º S under 'normal' and El Niño conditions [Dataset]. Deep Sea Research Part II: Topical Studies in Oceanography, *47*(9–11), 2101–2128. https://doi.org/10.1016/S0967-0645(00)00018-7

Hedges, J. I., Baldock, J. A., Gélinas, Y., Lee, C., Peterson, M., & Wakeham, S. G. (2001). Evidence for non-selective preservation of organic matter in sinking marine particles. *Nature*, *409*(6822), 801–804. https://doi.org/10.1038/35057247

Ichino, M. C., Clark, M. R., Drazen, J. C., Jamieson, A., Jones, D. O., Martin, A. P., et al. (2015). The distribution of benthic biomass in hadal trenches: A modelling approach to investigate the effect of vertical and lateral organic matter transport to the seafloor. *Deep Sea Research Part I: Oceanographic Research Papers*, *100*, 21–33. https://doi.org/10.1016/j.dsr.2015.01.010

Iversen, M. H., & Ploug, H. (2010). Ballast minerals and the sinking carbon flux in the ocean: Carbon-specific respiration rates and sinking velocity of marine snow aggregates. *Biogeosciences*, *7*(9), 2613–2624. https://doi.org/10.5194/bg-7-2613-2010

Jamieson, A. (2015). *The hadal zone: Life in the deepest oceans*. Cambridge University Press.

Kawagucci, S., Makabe, A., Kodama, T., Matsui, Y., Yoshikawa, C., Ono, E., et al. (2018). Hadal water biogeochemistry over the Izu–Ogasawara Trench observed with a full-depth CTD-CMS. *Ocean Science*, *14*(4), 575–588. https://doi.org/10.5194/os-14-575-2018

Kioka, A., & Strasser, M. (2022). Oceanic trenches. In *Treatise on geomorphology* (2nd ed., pp. 882–900). Academic Press. https://doi.org/10.1016/B978-0-12-818234-5.00167-X

Kong, L.-F., He, Y.-B., Xie, Z.-X., Luo, X., Zhang, H., Yi, S. H., et al. (2021). Illuminating key microbial Players and metabolic processes involved in the remineralization of particulate organic carbon in the Ocean's twilight zone by metaproteomics. *Applied and Environmental Microbiology*, *87*, 20–28. https://doi.org/10.1128/AEM.00986-21

Kriest, I. (2002). Different parameterizations of marine snow in a 1D-model and their influence on representation of marine snow, nitrogen budget and sedimentation. *Deep Sea Research Part I: Oceanographic Research Papers*, *49*(12), 2133–2162. https://doi.org/10.1016/S0967-0637(02)00127-9

Lee, C., Wakeham, S., & Arnosti, C. (2004). Particulate organic matter in the sea: The composition conundrum. *AMBIO: A Journal of the Human Environment*, *33*(8), 565–575. https://doi.org/10.1579/0044-7447-33.8.565

Liu, J., Zheng, Y., Lin, H., Wang, X., Li, M., Liu, Y., et al. (2019). Proliferation of hydrocarbon-degrading microbes at the bottom of the Mariana Trench. *Microbiome*, *7*(1), 1–13. https://doi.org/10.1186/s40168-019-0652-3

Liu, X., Wendt-Potthoff, K., Barth, J. A. C., & Friese, K. (2022). Post-depositional alteration of stable isotope signals by preferential degradation of algae-derived organic matter in reservoir sediments. *Biogeochemistry*, *159*(3), 315–336. https://doi.org/10.1007/s10533-022-00930-y

Luo, M., Gieskes, J., Chen, L., Scholten, J., Pan, B., Lin, G., & Chen, D. (2019). Sources, degradation, and transport of organic matter in the New Britain Shelf-Trench continuum, Papua New Guinea. *Journal of Geophysical Research: Biogeosciences*, *124*(6), 1680–1695. https://doi.org/10.1029/2018JG004691

Luo, M., Gieskes, J., Chen, L., Shi, X., & Chen, D. (2017). Provenances, distribution, and accumulation of organic matter in the southern Mariana Trench rim and slope: Implication for carbon cycle and burial in hadal trenches. *Marine Geology*, *386*, 98–106. https://doi.org/10.1016/j.margeo.2017.02.012

Luo, M., Glud, N. R., Pan, B., Wenzhöfer, F., Xu, Y., Lin, G., & Chen, D. (2018). Benthic carbon mineralization in hadal trenches: Insights from in-situ determination of benthic oxygen consumption. *Geophysical Research Letters*, *45*(6), 2752–2760. https://doi.org/10.1002/2017GL076232

Lutz, M. J., Caldeira, K., Dunbar, R. B., & Behrenfeld, M. J. (2007). Seasonal rhythms of net primary production and particulate organic carbon flux to depth describe the efficiency of biological pump in the global ocean. *Journal of Geophysical Research*, *112*(C10), C10011. https://doi.org/10.1029/2006JC003706

Lutz, M., Dunbar, R., & Caldeira, K. (2002). Regional variability in the vertical flux of particulate organic carbon in the ocean interior. *Global Biogeochemical Cycles*, *16*(3), 11–1. https://doi.org/10.1029/2000GB001383

Ma, J., Song, J., Li, X., Wang, Q., Zhong, G., Yuan, H., et al. (2021). The OMZ and its influence on POC in the tropical Western Pacific Ocean: Based on the survey in March 2018. *Frontiers in Earth Science*, *9*. https://doi.org/10.3389/feart.2021.632229

Martín, J., & Miquel, J.-C. (2010). High downward flux of mucilaginous aggregates in the Ligurian sea during summer 2002: Similarities with the mucilage phenomenon in the Adriatic sea. *Marine Ecology*, *31*(3), 393–406. https://doi.org/10.1111/j.1439-0485.2010.00361.x

Martin, J. H., Knauer, G. A., Karl, D. M., & Broenkow, W. W. (1987). VERTEX: Carbon cycling in the northeast Pacific. *Deep-Sea Research, Part A: Oceanographic Research Papers*, *34*(2), 267–285. https://doi.org/10.1016/0198-0149(87)90086-0

Matys, E., Sepúlveda, J., Pantoja, S., Lange, C., Caniupán, M., Lamy, F., & Summons, R. E. (2017). Bacteriohopanepolyols along redox gradients in the Humboldt current system off northern Chile. *Geobiology*, *15*(6), 844–857. https://doi.org/10.1111/gbi.12250

Menzel, D. W., & Ryther, J. H. (1968). Organic carbon and the oxygen minimum in the south Atlantic ocean. *Deep-Sea Research and Oceanographic Abstracts*, *15*(3), 327–337. Elsevier. https://doi.org/10.1016/0011-7471(68)90009-0

Meyers, P. A. (1994). Preservation of elemental and isotopic source identification of sedimentary organic matter. *Chemical Geology*, *114*(3–4), 289–302. doi:. https://doi.org/10.1016/0009-2541(94)90059-0

Meyers, P. A., & Eadie, B. J. (1993). Sources, degradation and recycling of organic matter associated with sinking particles in Lake Michigan. *Organic Geochemistry*, *20*(1), 47–56. https://doi.org/10.1016/0146-6380(93)90080-u

Middelburg, J., & Nieuwenhuize, J. (1998). Carbon and nitrogen stable isotopes in suspended matter and sediments from the Schelde Estuary. *Marine Chemistry*, *60*(3–4), 217–225. https://doi.org/10.1016/S0304-4203(97)00104-7

Middelburg, J. J. (2019). Carbon processing at the seafloor. In *Marine carbon biogeochemistry* (pp. 57–75). Springer. https://doi.org/10.1016/0146-6380(93)90080-U

Nakatsuka, T., Handa, N., Harada, N., Sugimoto, T., & Imaizumi, S. (1997). Origin and decomposition of sinking particulate organic matter in the deep water column inferred from the vertical distributions of its δ15N, δ13 and δ14. *Deep Sea Research Part I: Oceanographic Research Papers*, *44*(12), 1957–1979. https://doi.org/10.1016/S0967-0637(97)00051-4

Neubauer, D., Kolmakova, O., Woodhouse, J., Taube, R., Mangelsdorf, K., Gladyshev, M., et al. (2021). Zooplankton carcasses stimulate microbial turnover of allochthonous particulate organic matter. *The ISME Journal*, *15*(6), 1735–1750. https://doi.org/10.1038/s41396-020-00883-w

Oguri, K., Masqué, P., Zabel, M., Stewart, H. A., MacKinnon, G., Rowden, A. A., et al. (2022). Sediment accumulation and carbon burial in four hadal trench systems. *Journal of Geophysical Research: Biogeosciences*, *127*(10), e2022JG006814. https://doi.org/10.1029/2022JG006814

Oksanen, J., Blanchet, F. G., Kindt, R., Legendre, P., Minchin, P., O'hara, R., et al. (2013). Community ecology package. *R Package Version*, *2*(0).

Omand, M. M., D'Asaro, E. A., Lee, C. M., Perry, M. J., Briggs, N., Cetinić, I., & Mahadevan, A. (2015). Eddy-driven subduction exports particulate organic carbon from the spring bloom. *Science*, *348*(6231), 222–225.https://doi.org/10.1126/science.1260062

Omand, M. M., Govindarajan, R., He, J., & Mahadevan, A. (2020). Sinking flux of particulate organic matter in the oceans: Sensitivity to particle characteristics. *Scientific Reports*, *10*(1), 5582. https://doi.org/10.1038/s41598-020-60424-5

Pantoja, S., Sepúlveda, J., & González, H. E. (2004). Decomposition of sinking proteinaceous material during fall in the oxygen minimum zone off northern Chile. *Deep-Sea Research I*, *51*(1), 55–70. https://doi.org/10.1016/j.dsr.2003.09.005

Pavia, F. J., Anderson, R. F., Lam, P. J., Cael, B., Vivancos, S. M., Fleisher, M. Q., et al. (2019). Shallow particulate organic carbon regeneration in the South Pacific Ocean. Proceedings of the National Academy of Sciences, *116*(20), 9753–9758. [Dataset]. https://doi.org/10.1073/pnas.1901863116

Peterson, B. J., & Fry, B. (1987). Stable isotopes in ecosystem studies. *Annual Review of Ecology and Systematics*, *18*(1), 293–320. https://doi.org/10.1146/annurev.es.18.110187.001453

Pizarro, G., Iriarte, J. L., & Montecino, V. (2002). Mesoscale primary production and bio-optical variability off Antofagasta (23–24 S) during the transition to El Niño 1997–1998. *Revista Chilena de Historia Natural*, *75*(1), 201–215. https://doi.org/10.4067/S0716-078X2002000100019

Poff, K. E., Leu, A. O., Eppley, J. M., Karl, D. M., & DeLong, E. F. (2021). Microbial dynamics of elevated carbon flux in the open ocean's abyss. *Proceedings of the National Academy of Sciences*, *118*(4), e2018269118. https://doi.org/10.1073/pnas.201826911

Rafter, P. A., Bagnell, A., Marconi, D., & DeVries, T. (2019). Global trends in marine nitrate N isotopes from observations and a neural network-based climatology. *Biogeosciences*, *16*(13), 2617–2633. https://doi.org/10.5194/bg-16-2617-2019

Resplandy, L., Lévy, M., & McGillicuddy, D. J., Jr. (2019). Effects of eddy-driven subduction on ocean biological carbon pump. *Global Biogeochemical Cycles*, *33*(8), 1071–1084. https://doi.org/10.1029/2018GB006125

Rex, M. A., Etter, R. J., Morris, J. S., Crouse, J., McClain, C. R., Johnson, N. A., et al. (2006). Global bathymetric patterns of standing stock and body size in the deep-sea benthos. *Marine Ecology Progress Series*, *317*, 1–8. https://doi.org/10.3354/meps317001

Rice, A., Billett, D., Fry, J., John, A., Lampitt, R., Mantoura, R., & Morris, R. (1986). Seasonal deposition of phytodetritus to the deep-sea floor. *Proceedings of the Royal Society of Edinburgh - Section B: Biological Sciences*, *88*, 265–279. https://doi.org/10.1017/S0269727000004590

Ruiz-Fernández, P., Ramírez-Flandes, S., Rodríguez-León, E., & Ulloa, O. (2020). Autotrophic carbon fixation pathways along the redox gradient in oxygen-depleted oceanic waters. *Environmental Microbiology Reports*, *12*(3), 334–341. https://doi.org/10.1111/1758-2229.12837

Sauzède, R., Claustre, H., Uitz, J., Jamet, C., Dall'Olmo, G., d'Ortenzio, F., et al. (2016). A neural network-based method for merging ocean color and Argo data to extend surface bio-optical properties to depth: Retrieval of the particulate backscattering coefficient. *Journal of Geophysical Research: Oceans*, *121*(4), 2552–2571. https://doi.org/10.1002/2015JC011408

Schauberger, C., Seki, D., Cutts, E. M., Glud, R. N., & Thamdrup, B. (2023). Uniform selective pressures within redox zones drive gradual changes in microbial community composition in hadal sediments. *Environmental Microbiology*. https://doi.org/10.1111/1462-2920.16377

Selden, C. R., Mulholland, M. R., Widner, B., Bernhardt, P., & Jayakumar, A. (2021). Toward resolving disparate accounts of the extent and magnitude of nitrogen fixation in the Eastern Tropical South Pacific oxygen deficient zone. *Limnology & Oceanography*, *66*(5), 1950–1960. https://doi.org/10.1002/lno.11735

Siegel, D. A., Fields, E., & Buesseler, K. O. (2008). A bottom-up view of the biological pump: Modeling source funnels above ocean sediment traps. *Deep Sea Research Part I: Oceanographic Research Papers*, *55*(1), 108–127. https://doi.org/10.1016/j.dsr.2007.10.006

Srain, B. M., Sobarzo, M., Daneri, G., González, H., Testa, G., Farías, L., et al. (2020). Fermentation and anaerobic oxidation of organic carbon in the oxygen minimum zone of the upwelling ecosystem off concepción, in Central Chile. *Frontiers in Marine Science*, *7*, 533. https://doi.org/10.3389/fmars.2020.00533

Stock, B. C., Jackson, A. L., Ward, E. J., Parnell, A. C., Phillips, D. L., & Semmens, B. X. (2018). Analyzing mixing systems using a new generation of Bayesian tracer mixing models. *PeerJ*, *6*, e5096. https://doi.org/10.7717/peerj.5096

Suess, E. (1980). Particulate organic carbon flux in the oceans—Surface productivity and oxygen utilization. *Nature*, *288*(5788), 260–263. https://doi.org/10.1038/288260a0

Tamby, A., Sinninghe Damsté, J. S., & Villanueva, L. (2023). Microbial membrane lipid adaptations to high hydrostatic pressure in the marine environment. *Frontiers in Molecular Biosciences*, *9*, 1058381. https://doi.org/10.3389/fmolb.2022.1058381

Thamdrup, B., Schauberger, C., Larsen, M., Trouche, B., Maignien, L., Arnaud-Haond, S., et al. (2021). Anammox bacteria drive fixed nitrogen loss in hadal trench sediments. *Proceedings of the National Academy of Sciences*, *118*(46), e2104529118. https://doi.org/10.1073/pnas.2104529118

Turner, J. T. (2002). Zooplankton fecal pellets, marine snow and sinking phytoplankton blooms. *Aquatic Microbial Ecology*, *27*(1), 57–102. https://doi.org/10.3354/ame027057

Turnewitsch, R., Falahat, S., Stehlikova, J., Oguri, K., Glud, R. N., Middelboe, M., et al. (2014). Recent sediment dynamics in hadal trenches: Evidence for the influence of higher-frequency (tidal, near-inertial) fluid dynamics. *Deep Sea Research Part I: Oceanographic Research Papers*, *90*, 125–138. https://doi.org/10.1016/j.dsr.2014.05.005

Valdés, J., Sifeddine, A., Lallier-Verges, E., & Ortlieb, L. (2004). Petrographic and geochemical study of organic matter in surficial laminated sediments from an upwelling system (Mejillones del Sur Bay, Northern Chile). *Organic Geochemistry*, *35*(7), 881–894. https://doi.org/10.1016/j.orggeochem.2004.02.009

Van Mooy, B. A., Keil, R. G., & Devol, A. H. (2002). Impact of suboxia on sinking particulate organic carbon: Enhanced carbon flux and preferential degradation of amino acids via denitrification. *Geochimica et Cosmochimica Acta*, *66*(3), 457–465. https://doi.org/10.1016/S0016-7037(01)00787-6

Vargas, C. A., Cantarero, S. I., Sepúlveda, J., Galán, A., De Pol-Holz, R., Walker, B., et al. (2021). A source of isotopically light organic carbon in a low-pH anoxic marine zone [Dataset]. Nature Communications, *12*(1), 1604. https://doi.org/10.1038/s41467-021-21871-4

Wakeham, S. G., Lee, C., Farrington, J. W., & Gagosian, R. B. (1984). Biogeochemistry of particulate organic matter in the oceans: Results from sediment trap experiments [Dataset]. Deep-Sea Research, Part A: Oceanographic Research Papers, *31*(5), 509–528. https://doi.org/10.1016/0198-0149(84)90099-2

Warnes, G., Bolker, B., Bonebakker, L., Gentleman, R., Liaw, W., Lumley, T., & others (2015). gplots: Various R programming tools for plotting data. *R package version 2.16. 0*.

Weber, T., & Bianchi, D. (2020). Efficient particle transfer to depth in oxygen minimum zones of the Pacific and Indian Oceans. *Frontiers in Earth Science*, *8*, 376. https://doi.org/10.3389/feart.2020.00376

Wenzhöfer, F., Oguri, K., Middelboe, M., Turnewitsch, R., Toyofuku, T., Kitazato, H., & Glud, R. N. (2016). Benthic carbon mineralization in hadal trenches: Assessment by in situ O_2 microprofile measurements. *Deep Sea Research Part I: Oceanographic Research Papers*, *116*, 276–286. https://doi.org/10.1016/j.dsr.2016.08.013

Williams, J. R., & Giering, S. L. C. (2022). In situ particle measurements deemphasize the role of size in governing the sinking velocity of marine particles. *Geophysical Research Letters*, *49*(21), e2022GL099563. https://doi.org/10.1029/2022GL099563

Williams, P. M., & Gordon, L. I. (1970). Carbon-13: Carbon-12 ratios in dissolved and particulate organic matter in the sea. *Deep-Sea Research and Oceanographic Abstracts*, *17*(1), 19–27. https://doi.org/10.1016/0011-7471(70)90085-9

Xiao, W., Xu, Y., Haghipour, N., Montluçon, D. B., Pan, B., Jia, Z., et al. (2020). Efficient sequestration of terrigenous organic carbon in the New Britain Trench. *Chemical Geology*, *533*, 119446. https://doi.org/10.1016/j.chemgeo.2019.119446

Xu, Y., Ge, H., & Fang, J. (2018). Biogeochemistry of hadal trenches: Recent developments and future perspectives. *Deep Sea Research Part II: Topical Studies in Oceanography*, *155*, 19–26.https://doi.org/10.1016/j.dsr2.2018.10.006

Xu, Y., Li, X., Luo, M., Xiao, W., Fang, J., Rashid, H., et al. (2021). Distribution, source, and burial of sedimentary organic carbon in Kermadec and Atacama trenches. *Journal of Geophysical Research: Biogeosciences*, *126*(5), e2020JG006189. https://doi.org/10.1029/2020JG006189

Yuras, G., Ulloa, O., & Hormazábal, S. (2005). On the annual cycle of coastal and open ocean satellite chlorophyll off Chile (18–40 S). *Geophysical Research Letters*, *32*(23), L23604. https://doi.org/10.1029/2005GL023946

Zabel, M., Glud, R. N., Sanei, H., Elvert, M., Pape, T., Chuang, P.-C., et al. (2022). High carbon mineralization rates in subseafloor hadal sediments—Result of frequent mass wasting. *Geochemistry, Geophysics, Geosystems*, *23*(9), e2022GC010502.https://doi.org/10.1029/2022GC010502

Erratum

The originally published version of this article contained incomplete information about the co-authors. The affiliation for co-author Matías Pizarro-Koch should have included "[6]Escuela de Ingeniería Civil Oceánica, Facultad de Ingeniería, Universidad de Valparaíso, Valparaíso, Chile" which has now been added to the affiliations list. In the Author Contributions section, several authors were omitted inadvertently from the categories. The Conceptualization category has been corrected to: Igor Fernández-Urruzola, Sebastian I. Cantarero, Julio Sepúlveda, Osvaldo Ulloa. The Funding Acquisition category has been corrected to: Osvaldo Ulloa, Igor Fernández-Urruzola, Julio Sepúlveda. The Writing – Original Draft category has been corrected to: Igor Fernández, Sebastian I. Cantarero, Julio Sepúlveda. The Writing – Review & Editing category has been corrected to: Igor Fernández-Urruzola, Sebastian I. Cantarero, Matías Pizarro-Koch, Matthias Zabel, Julio Sepúlveda, Osvaldo Ulloa. These errors have now been corrected and this version may be considered the authoritative version of record.